Bilateral Teleoperation of Groups of Mobile Robots with Time-Varying Topology

Antonio Franchi, *Member, IEEE,* Cristian Secchi, *Member, IEEE,* Hyoung Il Son, *Member, IEEE,* Heinrich H. Bülthoff, *Member, IEEE,* and Paolo Robuffo Giordano, *Member, IEEE*

***Abstract*—In this paper, a novel decentralized control strategy for bilaterally teleoperating heterogeneous groups of mobile robots from different domains (aerial, ground, marine and underwater) is proposed. By using a decentralized control architecture, the group of robots, treated as the *slave-side*, is made able to navigate in a cluttered environment while avoiding obstacles, inter-robot collisions and following the human motion commands. Simultaneously, the human operator acting on the master side is provided with a suitable force feedback informative of the group response and of the interaction with the surrounding environment. Using passivity based techniques, we allow the behavior of the group to be as flexible as possible with arbitrary split and join events (e.g., due to inter-robot visibility/packet losses or specific task requirements) while guaranteeing the stability of the system. We provide a rigorous analysis of the system stability and steady-state characteristics, and validate performance through human/hardware-in-the-tloop simulations by considering a heterogeneous fleet of UAVs and UGVs as case study. Finally, we also provide an experimental validation with 4 quadrotor UAVs.**

***Index Terms*—Distributed Robot Systems, Telerobotics, Networked Robots, Teleoperation of Mobile Robots, Multi-robot systems, Mobile agents, Distributed algorithms, Decentralized control, Haptics, Passivity-based control.**

I. Introduction

FOR several applications like surveillance of large perimeters, search and rescue in disaster regions, and exploration of wide or unaccessible areas, the use of a group of simple robots rather than a single complex robot has proven to be very effective, and the problem of coordinating a group of agents has received a lot of attention by the robotics and control community over the last decade, see [1] for a survey. Indeed, such a fruitful interplay has resulted in significant advances in the mathematical formalization, theoretical analysis and actual realization of complex multi-robot systems for diverse applications, like exploration [2], coverage [3], and cooperative transportation [4]. Nevertheless, when the tasks become extremely complex and high-level cognitive-based decisions are required online, complete autonomy is still far from being reached. In this context, teleoperation systems, where a human operator commands a remote robot through a local interface, can be used to exploit human's intelligence.

In this paper, we study the problem of establishing a *bilateral* teleoperation system for remotely controlling, in a decentralized way, the motion of a heterogeneous group of mobile robots, such as aerial, ground, space, naval, or underwater vehicles. Indeed, the fundamental problem addressed in this work consists of establishing a bilateral teleoperation channel for remote *navigation* purposes, i.e., a necessary premise for any other specific objective, such as tele-exploration, -transport, or -manipulation. In our envisaged teleoperation system, the remote mobile robots (the *slave-side* from now on) should possess some minimum level of local autonomy and act as a *group*, e.g., by maintaining some desired inter-distances and avoiding collisions by means of decentralized controllers. At the same time, the human operator, acting on the *master device*, should be in control of the overall group motion and receive, through haptic feedback, suitable cues informative enough of the remote robot/environment state. On top of this remote navigation layer, the group should still be allowed to perform additional local tasks by exploiting the internal slave side redundancy w.r.t. the master device commands.

Bilateral teleoperation of (multiple) mobile robots presents several differences w.r.t. conventional teleoperation systems: first, there exists a structural *kinematic dissimilarity* between master and slave sides, i.e., the master possesses a limited workspace while the slave an unbounded one. Second, in a typical scenario, there is no physical contact with the environment since this would represent a dangerous situation (e.g., a crash) for the robots. Lastly, the slave-side possesses large motion redundancy w.r.t. the master-side because of the gap between the degrees of freedom (DOFs) of the master (usually in the range of 3–6), and the DOFs of the slave (in the range of $6N$ for N robots, when considered as rigid bodies). A proper design of a multi-robot slave-side must also cope with the typical requirements of *decentralized sensing and control* for guaranteeing robustness to failures, achieving actual feasibility, and ensuring low computational load: roughly speaking, one should avoid the presence of any central sensing, communication or control unit in the network [1], [5]. Finally, the design of a navigation-oriented teleoperation should allow for the possibility of adding extra-tasks independent of the

Manuscript received XXXX XX, XXXX; revised XXXXXX XX, XXX; accepted November XX, XXXX. This paper was recommended for publication by Associate Editor X. X. XXXXXX and Editor XXXX XXXXXXXXX upon evaluation of the reviewers comments.

A. Franchi, H. I. Son, and P. Robuffo Giordano are with the Max Planck Institute for Biological Cybernetics, Spemannstraße 38, 72076 Tübingen, Germany {antonio.franchi, hyoungil.son, prg}@tuebingen.mpg.de.

C. Secchi is with the Department of Science and Methods of Engineering, University of Modena and Reggio Emilia, via G. Amendola 2, Morselli Building, 42122 Reggio Emilia, Italy cristian.secchi@unimore.it

H. H. Bülthoff is with the Max Planck Institute for Biological Cybernetics, Spemannstraße 38, 72076 Tübingen, Germany, and with the Department of Brain and Cognitive Engineering, Korea University, Anam-dong, Seongbuk-gu, Seoul, 136-713 Korea hhb@tuebingen.mpg.de.

Color versions of one or more of the figures in this paper are available online at http://ieeexplore.ieee.org.

Digital Object Identifier XXXXXXXXXXXXXXXXXXXXXXXX

main navigation command received from the human operator. Therefore, stability w.r.t. time-varying interaction topology within the slave side network should also be granted.

A. Contribution and Relation to Previous Work

A lot of interest is recently arising in the robotics community in the bilateral teleoperation of mobile robots, see, for instance, [6], [7], [8], where the haptic teleoperation of a *single* mobile robot is considered. In fact, it has been widely proven that the use of a force information allows to obtain superior performance with respect to the case where no haptic feedback is present, see, e.g., [9], [10], [11], [12].

In [13], a conventional multi-master/multi-slave teleoperation system with no delay is developed and a centralized strategy for controlling the cooperative behavior of the robots is proposed. In [14], [15], two approaches for controlling multiple ground robots through a master device are presented, while in [16], an impedance controller for teleoperating a group of slaves in a leader-follower modality is proposed. Finally, in [17], a bilateral control strategy that allows to coordinate the motion between the master and the slaves under arbitrary time delay is proposed, while in [18] a related (still passivity-based) work that considers fixed topology and deformable but fixed shape is also presented. The main limitations of these approaches are the centralization (every robot needs to communicate with the master and/or with all the other robots), and the rigidity of the fleet which is not allowed, for example, to actively reshape the formation or to vary its topology online because of (arbitrary) internal decisions. Moreover, some of the cited works do not address the master/slave kinematic dissimilarity and consider a standard position-position teleoperation architecture which is not particularly suited for a bilateral teleoperation of *mobile robots*.

Many existing leader-follower concepts could be seen as examples of *unilateral* teleoperation of multiple mobile robots (e.g., see [5], [19]). Nevertheless, *bilateral* teleoperation does not constitute a straightforward extension because of the additional coupling between the motion of the slave and the forces applied to the master device. Finally, similarly to our work, in [20] the possibility of splitting or joining the formation for double-integrator agents is also considered. However, the authors considered the possibility of splits and joins *only* for excessive inter-robot distances: from the slave-side stability point of view, this is a quite simplified situation w.r.t. the case considered in this work where split and join decisions can be taken *at any time* and because of *any internal criterium*, see Rem. 4 in Sect. II-A for more details.

To the best of our knowledge, this paper is the first attempt in proposing a framework able to address most of the aforementioned points by implementing a bilateral teleoperation system for remotely controlling a group of robots in a highly flexible and decentralized way. The theoretical foundation on top of which the paper is built is passivity-based control: on one side, passivity theory is exploited for guaranteeing a stable behavior of the slave group *per se* despite of autonomous maneuvers, time-varying fleet topology, and interaction with remote obstacles in a clean and powerful manner. On the other side, passivity theory is also instrumental for characterizing the stability of the 'feedback interconnection' among the environment/slave-side/master-side/human-operator as classically done in many previous teleoperation works [21].

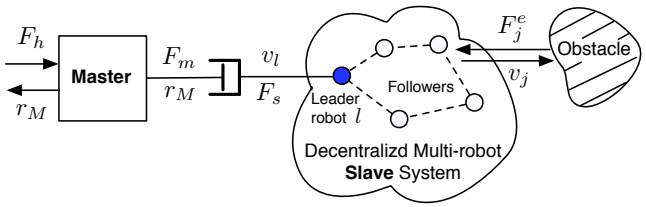

Fig. 1: The overall teleoperation system. From left to right: F_h is the human operator force applied to the master device; r_M is a velocity-like quantity which is almost proportional to the position of the haptic device; F_m is the control force applied to the master in order to provide haptic feedback; v_l is the velocity of the leader and F_s is a force applied to the leader to make it follow the desired velocity; finally v_j is the velocity of a generic j-th robot and F_j^{env} is its interaction force with the external environment (obstacles).

The foundations of this approach, presented in [22], have been extended in this paper by adding the the steady-state analysis; improving the presentation, motivations, theory, and reference to related works; performing more thorough human/hardware-in-the-loop simulations; and adding an experiment with a group of 4 real quadrotor UAVs.

The paper is organized as follows: after presenting the architecture in Sec. II, Sec. II-A introduces one of the main contributions of the paper, i.e., a passivity-based modeling of the group of mobile robots and its interaction with the environment. Then, Sec. II-B and II-C describe the master-device model and the master/slave passive interconnection, respectively. Sec. III formally characterizes the steady-state regime. Finally, human/hardware-in-the-loop simulations using UAVs (quadrotors) and UGVs (differentially driven wheeled robots) are reported in Sec. IV, as well as experiments obtained with 4 quadrotor UAVs. Section V concludes the paper and discusses future research directions.

II. The Teleoperation System

For the reader's convenience, we will informally summarize the architecture of our teleoperation system which will be then rigorously detailed in the next Sects. II-A, II-B, and II-C. In our scheme, depicted Fig. 1, the slave side consists of a group of N agents among which a *leader* is chosen (denoted by the subscript l). The motion of an agent depends on the motion of the locally surrounding agents and obstacles by means of the action of *nonlinear elastic-like couplings*. The leader is a special agent that is also subject to the master control represented by the additional external force F_s. The remaining agents (not controlled by the master) are referred to as *followers*. The spring coupling between a pair of agents can be broken and/or re-established at any time. In this way, we ensure high flexibility w.r.t. possible additional tasks, and adequate maneuverability within cluttered environments as the group shape does not result overly constrained. The design and

stability analysis of the slave side is thoroughly illustrated in Sec. II-A and represents a major contribution of this paper.

The velocity-like quantity r_M, (almost) proportional to the position of the master device, acts as velocity setpoint for the leader at the slave side thanks to the master/slave coupling force F_s (as explained in Sec. II-C). This allows to address the aforementioned master-slave kinematic dissimilarity. Conversely, the mismatch between r_M and the actual leader velocity v_l is transformed into the force F_m at the master side, in order to transmit to the user a feeling of the remote side (see Sec. II-B). This force will be shown in Sec. III to carry information about the total number and velocity of agents in the group, and about the interaction with the surrounding environment because of the leader-followers mutual influence.

Passivity will be the leitmotif throughout the whole design and analysis phase. In fact, in order to ensure the stability of the system, our primary goal will be to design the master and slave side as passive systems joined by a passive interconnection. In this way, the bilateral teleoperation system will be characterized by a stable behavior in case of interaction with passive environments and passive human users. The choice of relying on the passivity framework is motivated by the following reasons: (i) in classical bilateral teleoperation settings, passivity is a well-established tool for proving stability of the human/master/slave/environment interconnection, see [21], [23] for a survey; (ii) because of the flexible behavior that will be described in Sect. II-A, the slave-side behaves as a switching system. Passivity provides a powerful and elegant tool to enforcing its stability under arbitrary switching (see `PassiveJoin` Procedure in Sec. II-A), while, if not using passivity, one should *still* design other strategies for guaranteeing stability of the slave-side switching dynamics; (iii) finally, providing a strategy that could make the slave-side stable but *not* passive would nullify the benefits discussed in point (i). Indeed, in this case one should explicitly prove the stability of the master/slave feedback interconnection rather than exploiting the well-known result of stable interconnection of a (passive) master with a (passive) slave.

Finally, note that the leader can be any robot in communication with the master side — the only requirement is that such a robot does exist at all times. Nevertheless, any specific strategy for choosing the leader robot can also be adopted depending on the particular application or task. For instance, [24] illustrates a way to choose a leader by maximizing the tracking performance of the slave.

A. The Slave Side

The slave side consists of a group of N robots coupled together. In this Section we detail a control strategy for obtaining a flexible cohesive behavior of the group (i.e., allowing arbitrary split and join) and, at the same time, to avoid inter-robot and obstacle collisions.

Every agent is modeled as a floating mass in $\mathbb{R}^3$, that is, an element storing kinetic energy:

$$\begin{cases} \dot{p}_i = F_i^a + F_i^e - B_i M_i^{-1} p_i \\ v_i = \frac{\partial \mathcal{K}_i}{\partial p_i} = M_i^{-1} p_i \end{cases} \qquad i = 1, \ldots, N \quad (1)$$

where $p_i \in \mathbb{R}^3$ and $M_i \in \mathbb{R}^{3\times 3}$ are the momentum and (symmetric positive definite) inertia matrix of agent i, respectively, $\mathcal{K}_i = \frac{1}{2} p_i^T M_i^{-1} p_i$ is the kinetic energy stored by the agent during its motion, and $B_i \in \mathbb{R}^{3\times 3}$ is a positive definite matrix representing an artificial damping added for asymptotically stabilizing the behavior of the agent[1]. Force $F_i^a \in \mathbb{R}^3$ represents the interaction of agent i with the other agents and will be designed in the following, while $F_i^e \in \mathbb{R}^3$ represents the interaction of agent i with the 'external world', i.e., the environment (obstacles) and the master side through the teleoperation channel (Sec. II-C). Finally, $v_i \in \mathbb{R}^3$ is the velocity of the agent, and $x_i \in \mathbb{R}^3$ its position, with $\dot{x}_i = v_i$.

Note that terms M_i allow to model different inertial properties depending on the direction of motion (e.g., a quadrotor whose vertical dynamics is usually faster than the horizontal one). Furthermore, we can enforce heterogeneity in the group by providing different inertial characteristics $M_1, \ldots, M_N$ and fluid resistances $B_1, \ldots, B_N$ (e.g., aerodynamic versus hydrodynamic drag).

Remark 1. *Depending on the context,* (1) *can be easily recast in* $\mathbb{R}^2$ *to, e.g., model ground or naval vehicles by properly including those reaction forces arising from the presence of geometrical constraints (e.g., when motion is bound to a planar surface). We also assume that the robots under consideration are endowed with a controller able to track the smooth Cartesian trajectory generated by* (1) *with small/negligible tracking errors. This is the case, for example, of all the systems with a cartesian flat output [25], i.e., a point in* $\mathbb{R}^3$ *that algebraically defines, with its derivatives, the state and the control inputs of the system. Many mobile robots, including the usual nonholonomic ground robots, exhibit this property: for instance, [26] gives a non-exhaustive list of differentially flat mechanical systems such as nonholonomic vehicles or submarines. However, the description of particular trajectory tracking controllers is outside the scope of this paper, e.g., see [27] where a related control strategy for a class of UAVs is discussed*[2].

The following definition will be used later on to define a suitable interaction graph for the group.

Definition 1 (Neighboring Agents)**.** *Let* $d_{ij} = \|x_i - x_j\|$ *be the inter-distance among agents* i *and* j*, and* $\sigma_{ij}(t) : \mathbb{R} \to \{0, 1\}$*,* $i \neq j$*, represent a time-varying boolean condition satisfying* at least *the following requirements:*

1) $\sigma_{ij}(t) = 0$*, if* $d_{ij} > D \in \mathbb{R}^+$*;*
2) $\sigma_{ij}(t) = \sigma_{ji}(t)$*.*

Then, two agents i *and* j *are defined as being* neighbors *if and only if* $\sigma_{ij}(t) = 1$*. Furthermore, two agents* i *and* j *are said to* join *if they become neighbors (*$\sigma_{ij} = 0 \to \sigma_{ij} = 1$*) and, conversely, are said to* split *if they become non-neighbors (*$\sigma_{ij} = 1 \to \sigma_{ij} = 0$*).*

[1] This can also represent typical physical phenomena, e.g., wind/atmosphere drag for UAVs, or hydrodynamic drag for underwater robots.

[2] Alternatively, one could track the flow of (1) with a feedback-linearizable Cartesian output of the robotic system under consideration (e.g., a point off the mid-axle position in differentially driven ground robots). This technique is exploited in [28].

This neighboring definition is purposely stated in a very general form in order to account for any additional task requirement independent of the main navigation command. In this sense, item 1) is meant to model a generic limited range capability of onboard sensors and/or communication complexity of the robot network: whatever the task at hand, two agents are never allowed to interact if their interdistance overcomes a certain threshold D. However, Def. 1 also leaves the possibility for a $\sigma_{ij}(t) = 0$ even though $d_{ij} \leq D$. This captures our intention of admitting the presence of additional subtasks or constraints the agents may be subject to during their motion. For instance, in our teleoperation framework, the fleet could decide to separate in different logical subgroups in order to accomplish different objectives, but the separation decision could take place when the interdistances are less than D. Similarly, the agents could be equipped with sensors not always able to provide their mutual position even if $d_{ij} < D$ (e.g., visibility sensors such as cameras affected by occlusions, or wireless communication undergoing temporary packet losses), resulting in unwanted but unavoidable disconnections with their neighbors. Nevertheless, when two agents are actually interacting, we also require that they keep some preferred interdistance in order to avoid collisions and to achieve a cohesive behavior of the fleet. Finally, item 2) represents the fact that we aim for a *symmetric* neighboring condition: two agents always agree on their interaction state.

According to Def. 1, we then denote with $\mathcal{N}_i$ the set of neighbors of i. Since the relationship is symmetrical, $j \in \mathcal{N}_i \Leftrightarrow i \in \mathcal{N}_j$. Finally, we also denote with $\mathcal{G}(t) = (\mathcal{V}, \mathcal{E}(t))$ the undirected graph induced by this neighboring relationship where the vertices $\mathcal{V}$ represent the agents and $\mathcal{E}(t) = \{(i,j) \in \mathcal{V} \times \mathcal{V} \,|\, \sigma_{ij}(t) = 1 \Leftrightarrow j \in \mathcal{N}_i\}$.

1) Inter-Agent Coupling: We now define the interaction force acting among two neighboring agents. In order to achieve a collision-free, flexible and cohesive behavior of the fleet, we take inspiration from the inter-agent coupling proposed in [5] which, in turn, stemmed from the natural behavior of flocks of animals [29]. Let $d_0 < D$ be a desired distance between the agents. If $j \in \mathcal{N}_i$, agent i computes an interaction force F_{ij}^a whose magnitude and direction depends on the relative distance d_{ij} and bearing $\eta_{ij} := (x_i - x_j)/d_{ij}$ between i and j. In particular, the force is always directed along the bearing: if $d_{ij} < d_0$ a repulsive force is generated; if $d_{ij} = d_0$ a null force is produced; and if $d_0 < d_{ij} \leq D$ an attractive force is computed. We also assume that, if $d_{ij} > D$, a null force is generated since in this case $j \notin \mathcal{N}_i$ by definition. Notice that, according to the previous definitions, it is $F_{ij}^a = -F_{ji}^a$.

This inter-agent coupling can be modeled as the gradient of a nonlinear elastic element (virtual spring) that interconnects a pair of agents whenever they are neighbors. A possible potential function $\bar{V}(d_{ij})$ with such a desired behavior is shown in Fig. 2. Note that the shape of the potential goes to infinity as d_{ij} approaches zero for providing an effective inter-agent repulsive force[3]. As proposed in [30], we then model the elastic coupling between two agents i and j as a (potential)

[3]In general, any lower bounded potential (e.g., the one proposed in [17]) having similar features would be a suitable choice.

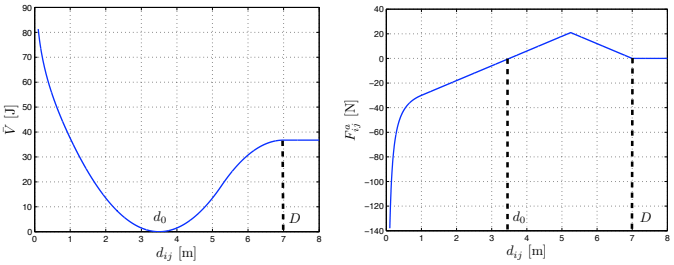

Fig. 2: The shape of the interagent potential as a function of the distance (left), and the corresponding coupling force (right)

energy storing element

$$\begin{cases} \dot{x}_{ij} = v_{ij} \\ F_{ij}^a = \frac{\partial V(x_{ij})}{\partial x_{ij}} \end{cases} \tag{2}$$

where $x_{ij}, v_{ij}, F_{ij}^a \in \mathbb{R}^3$ are, respectively, the state, the input, and the output (i.e., the generated force) of the virtual spring, and $V(x_{ij}) = \bar{V}(\|x_{ij}\|)$ is the spring energy function.

Whenever $j \in \mathcal{N}_i$, the virtual coupling (2) is connected (i.e., exchanges energy) with the dynamics (1) of agents i and j. This formally means that the state x_{ij} is initialized to $x_i - x_j$, $v_{ij} = \dot{x}_i - \dot{x}_j = v_i - v_j$ in (2), and F_{ij}^a contributes to F_i^a in (1) as:

$$F_i^a = \sum_{j \in \mathcal{N}_i} F_{ij}^a := \sum_{j \in \mathcal{N}_i} \frac{\partial \bar{V}}{\partial d_{ij}} \frac{\partial d_{ij}}{\partial x_{ij}} = \sum_{j \in \mathcal{N}_i} \frac{\partial \bar{V}}{\partial d_{ij}} \eta_{ij}. \tag{3}$$

Symmetrically, when $j \notin \mathcal{N}_i$, the virtual coupling is disconnected from the agent dynamics, that is, $v_{ij} = 0$ and F_{ij}^a does not contribute to F_i^a.

Remark 2. *We note that the interaction force F_i^a can be computed by agent i in a decentralized way. In fact, the computation is based on the shape of the inter-agent potential (which is known from the design phase), and on the distance and bearing of agents $j \in \mathcal{N}_i$ w.r.t. agent i.*

In order to write the overall agent/spring dynamics (slave-side) in a compact form, define $p = (p_1^T, \ldots, p_N^T)^T \in \mathbb{R}^{3N}$, $B = diag(B_i) \in \mathbb{R}^{3N \times 3N}$, $x = (x_{12}^T, \ldots, x_{1N}^T, x_{23}^T, \ldots, x_{2N}^T, \ldots, x_{N-1N}^T)^T \in \mathbb{R}^{\frac{3N(N-1)}{2}}$ and $F^e = (F_1^{eT}, \ldots, F_N^{eT})^T \in \mathbb{R}^{3N}$, and let $\mathcal{I}_{\mathcal{G}}(t) \in \mathbb{R}^{N \times \frac{N(N-1)}{2}}$ be the incidence matrix of the graph $\mathcal{G}(t)$ with the edge numbering and orientation induced by the entries of vector x. Notice that $\mathcal{I}_{\mathcal{G}}(t)$ has a constant size despite of the time-varying nature of $\mathcal{G}(t)$. Indeed, $j \notin \mathcal{N}_i$ will result in a column of all zeros for $\mathcal{I}_{\mathcal{G}}(t)$ in correspondence of the edge (i,j). It is then possible to model the slave side as a mechanical system described by:

$$\begin{cases} \begin{pmatrix} \dot{p} \\ \dot{x} \end{pmatrix} = \left[\begin{pmatrix} 0 & \mathcal{I}(t) \\ -\mathcal{I}^T(t) & 0 \end{pmatrix} - \begin{pmatrix} B & 0 \\ 0 & 0 \end{pmatrix} \right] \begin{pmatrix} \frac{\partial H}{\partial p} \\ \frac{\partial H}{\partial x} \end{pmatrix} + GF^e \\ v = G^T \begin{pmatrix} \frac{\partial H}{\partial p} \\ \frac{\partial H}{\partial x} \end{pmatrix} \end{cases} \tag{4}$$

where

$$H = \sum_{i=1}^{N} \mathcal{K}_i + \sum_{i=1}^{N-1} \sum_{j=i+1}^{N} V(x_{ij}) \tag{5}$$

is the total energy of the system, $\mathcal{I}(t) = \mathcal{I}_{\mathcal{G}}(t) \otimes I_3$, and $G = \left((I_N \otimes I_3)^T \quad 0^T\right)^T$, with I_3 and I_N being the identity matrices of order 3 and N respectively, 0 representing a null matrix of proper size, and $\otimes$ denoting the Krönecker product.

Proposition 1. *Assuming $\mathcal{I}(t) = const$, i.e., no splits and joins are taking place because $\sigma_{ij}(t) \equiv const\ \forall i, \forall j \neq i$, system (4) is passive with respect to the input/output pair (F^e, v) with storage function H.*

Proof: The potential reported in Fig. 2 is a lower bounded function of the scalar distance among the agents $\|x_{ij}\|$ and, as a consequence, a lower bounded function of x_{ij}. By evaluating the time derivative of the storage function (5) $\dot{H} = \begin{pmatrix} \frac{\partial^T H}{\partial p} & \frac{\partial^T H}{\partial x} \end{pmatrix} \begin{pmatrix} \dot{p} \\ \dot{x} \end{pmatrix}$ along the system trajectories in (4), and by noting that B is positive definite, it follows that

$$\dot{H} = -\frac{\partial^T H}{\partial p} B \frac{\partial H}{\partial p} + v^T F^e \leq v^T F^e \tag{6}$$

which concludes the proof. ■

Since (4) is a passive system, its interaction with any passive environment will still preserve passivity. This easily allows to include in inputs F_i^e in (1) an obstacle avoidance action. Indeed, as usual in applications involving mobile agents in unknown environments, we assume that, when they are detected, obstacles are treated as repulsive potentials producing a force that vanishes if the robot is far enough and grows as the robot comes closer to the obstacle. Such potentials can also be modeled as virtual springs, that is, passive systems, and their action is considered to be embedded in the terms F_i^e

2) Split and Join While Preserving the Slave-Side Passivity: Having established passivity of the slave-side with a constant interaction graph topology $\mathcal{G} = const$, we now analyze the general case of a time-varying $\mathcal{G}(t)$ because of the join and split decisions of Def. 1.

Proposition 2. *If two agents i and j split according to Def. 1, then passivity of* (4) *is preserved.*

Proof: If agent i and agent j split, the behavior of the slave side can be described by a subgraph of $\mathcal{G}$, $\mathcal{G}' = (\mathcal{V}', \mathcal{E}')$, where $\mathcal{V}' = \mathcal{V}$ and $\mathcal{E}'$ is obtained by $\mathcal{E}$ by erasing the edge connecting vertex i with vertex j. The behavior of the slave side in case of split can be modeled by replacing, in (4), the incidence matrix $\mathcal{I}$ with a new incidence matrix $\mathcal{I}' = \mathcal{I}_{\mathcal{G}'} \otimes I_3$. The passivity of the system then follows from the same arguments of Proposition 1. ■

Remark 3. *The fact that passivity of the slave-side is preserved despite of changes in $\mathcal{I}$ in* (4) *due to split decisions depends on the fact that $\mathcal{I}$ enters in the definition of a skew-symmetric matrix which leads to a null term in the energy balance* (6)*. Also, during a split between two agents i and j, the elastic element x_{ij} becomes isolated from the dynamics of the agents and keeps on storing the same energy $V(x_{ij})$ that was storing before the split decision, while the agents keep on interacting with the rest of the system.*

A join decision, on the other hand, can lead to a violation of the slave side passivity: allowing two agents to join means instantaneously switching from a state characterized by no interaction to the inter-agent interaction of (2). This results in a new edge in $\mathcal{E}$, and in a corresponding update of the overall incidence matrix $\mathcal{I}$. While, as per Prop. 2, a change in $\mathcal{I}$ does not threaten passivity, some extra energy can still be produced during the join procedure. In fact, in the general case, the relative distance of two agents at the join decision can be different from their relative distance at the split decision, and this can result in a non passive behavior as shown in the illustrative example of Fig. 3 where some extra energy is produced when the agents join.

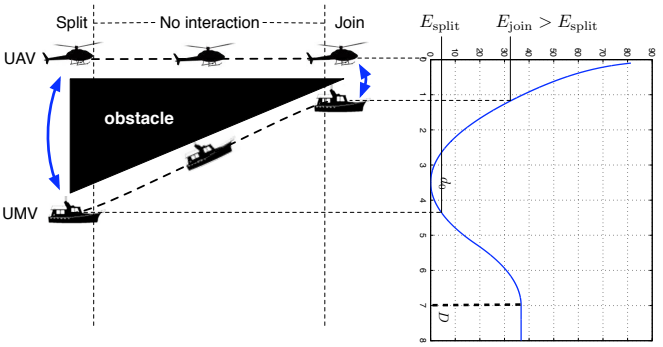

Fig. 3: When the agents (e.g., a UAV and a Marine Vehicle) split, the energy E_{split} is stored in the spring, while when they join the energy $E_{\text{join}} > E_{\text{split}}$ is needed to implement the new desired coupling. In this case, without proper strategies, an amount $E_{\text{join}} - E_{\text{split}} > 0$ of energy would be introduced into the system, thus violating passivity.

Remark 4. *Note that in the particular case of a split because $d_{ij} > D$ followed by a join because $d_{ij} = D$ (see Def. 1), the join decision never threatens passivity: indeed, when the two agents split it is $\bar{V}(d_{ij}) = \bar{V}(D)$ and, necessarily, when they join it is again $\bar{V}(d_{ij}) = \bar{V}(D)$. Therefore, no extra energy is produced in this case.*

In order to implement the join procedure in a passive way, we then propose to keep track of the energy dissipated by each agent: to this end, we introduce a local variable $t_i \in \mathbb{R}$, called *tank*, along with an associated energy function $T_i = \frac{1}{2} t_i^2$ for storing the energy dissipated by the agent. This energy reservoir can then be used for compensating excess of energy in the slave side and, thus, for implementing join decisions without violating the passivity of the system. Using (1), the power dissipated by agent i because of the damping is

$$D_i = p_i^T M_i^{-T} B_i M_i^{-1} p_i. \tag{7}$$

Considering the tank variables, we then adopt the following extended dynamics for the agents and elastic elements:

$$\begin{cases} \dot{p}_i = F_i^a + F_i^e - B_i M_i^{-1} p_i \\ \dot{t}_i = (1 - \beta_i) \left(\alpha_i \frac{1}{t_i} D_i + \sum_{j=1\ldots N, j \neq i} w_{ij}^T F_{ij}^a \right) + \beta_i c_i \\ y_i = \begin{pmatrix} M_i^{-1} p_i \\ t_i \end{pmatrix} \end{cases} \tag{8}$$

$$\begin{cases} \dot{x}_{ij} = v_{ij} - w_{ij} t_i + w_{ji} t_j \\ F_{ij}^a = \dfrac{\partial V(x_{ij})}{\partial x_{ij}} \end{cases} \tag{9}$$

The quantity $\alpha_i \in \{0,1\}$ is a design parameter that disables/enables the storage of D_i, the energy dissipated by the system. The quantity $\beta_i \in \{0,1\}$ is a design parameter which allows to switch the behavior of the tank element from a *storage mode* (i.e., the energy dissipated by the agent is stored) to a *consensus mode* (i.e., a consensus algorithm is run among the tanks). The role of inputs $w_{ij} \in \mathbb{R}^3$ is to allow for an energy exchange among the tank energy T_i and the elastic elements $V(x_{ij})$. Indeed, by setting

$$w_{ij} = \gamma_{ij}(1-\beta_i)t_i F^a_{ij}, \tag{10}$$

where $\gamma_{ij} \in \mathbb{R}$ is a modulation parameter, it is possible to implement a *lossless energy transfer* among the storages T_i and $V(x_{ij})$ [8], [31]. In particular, if $\gamma_{ij} > 0$, some energy is extracted from $V(x_{ij})$ and injected into T_i, while the opposite behavior is obtained with $\gamma_{ij} < 0$. The magnitude of γ_{ij} dictates the rate of this exchange, with $\gamma_{ij} = 0$ implying no energy exchange taking place. Note that, while by construction it is $F^a_{ij} = -F^a_{ji}$, in general $w_{ij} \neq w_{ji}$ and $\gamma_{ij} \neq \gamma_{ji}$. Furthermore, in order to comply with our decentralization guidelines, in (8) we allow for a $\gamma_{ij} \neq 0$ only if $j \in \mathcal{N}_i$. The use of w_{ij} will be illustrate later on.

When the system is in storage mode ($\beta_i = 0$), we have that:

$$\dot{T}_i = \alpha_i D_i + t_i \sum_{j \in \mathcal{N}_i} w^T_{ij} F^a_{ij}. \tag{11}$$

If $\alpha_i = 1$ and $\gamma_{ij} = 0$, all the energy dissipated because of the damping injection on the dynamics of agent i is stored back into the tank. This is the energy that can be "used" in the system without violating the passivity constraint. Because of the reasons reported in [32], it is wise to disable the energy storage for avoiding an excess of internal energy that would allow to implement unstable behaviors in the system. Thus, we set:

$$\alpha_i = \begin{cases} 0 & \text{if } T_i \geq \bar{T}_i \\ 1 & \text{otherwise} \end{cases}. \tag{12}$$

where $\bar{T}_i$ is a proper bound to be selected depending on the particular application. In order to avoid singularities in (8) (i.e., $t_i = 0$), we also set a threshold $\varepsilon > 0$ below which it is forbidden to extract energy from the tank.

When the system switches to consensus mode ($\beta_i = 1$), the terms c_i are used for redistributing the energy among the tanks. A decentralized strategy is implemented for equally leveling the energy stored in the tanks just before the join. This is done by running a consensus algorithm [1]

$$\dot{T}_i = -\sum_{j \in \mathcal{N}_i} (T_i - T_j) \tag{13}$$

Such energy redistribution can be implemented acting on the variable t_i. In fact, since $\dot{T}_i = \dot{t}_i t_i$, (13) is equivalent to setting in (8)

$$c_i = -\frac{1}{t_i} \sum_{j \in \mathcal{N}_i} (T_i(t_i) - T_j(t_j)). \tag{14}$$

We will now detail a strategy, called `PassiveJoin` Procedure, to allow for a safe implementation of join decisions. When agent i and j split, the one with the lower ID between i and j stores x_{ij} in a local variable x^s_{ij} which represents the state of the virtual spring at the split time. If agents i and j never split before, x^s_{ij} is initialized such that $V(x^s_{ij}) = \bar{V}(D) = \bar{V}_{ij}(\infty)$. When two agents i and j want to join, the `PassiveJoin` Procedure is preliminary run on agent i (and on agent j with proper modifications on the notation), and the actual join decision (i.e., the update of matrix $\mathcal{I}$) is slightly postponed after its completion. The procedure requires x^s_{ij} (which is shared by the agent with lower ID via local communication) and x_j and t_j that can be sent via local communication by agent j to agent i. First, agent i computes the quantity $\Delta E = V(x_i - x_j) - V(x^s_{ij})$ (line 1). If $\Delta E \leq 0$, the energy needed for implementing the join is lower than the energy previously stored in the spring and, therefore, the join process is actually dissipating energy. Half of the dissipated energy, $(-\Delta E)/2$, can be stored back in the tank of agent i by means of the input w_{ij} (line 3), and the other half will be stored in the tank of the agent j by means of the input w_{ji}. Then, the agents can safely join (line 9)[4].

Procedure PassiveJoin

```
   Data: x_i, x_j, x^s_ij, t_i, t_j
1  Compute ΔE = V(x_i − x_j) − V(x^s_ij);
2  if ΔE ≤ 0 then
3      Store (−ΔE)/2 in the tank through input w_ij;
   else
4      if T_i(t_i) + T_j(t_j) < ΔE + 2ε then
5          Run a consensus on the tank variables;
6          if 2T_i(t_i) < ΔE + 2ε then
7              Dampen until T(t_i) + T(t_j) ≥ ΔE + 2ε;
8      Extract T(t_i)/(T(t_i) + T(t_j)) ΔE from the tank through input w_ij;
9  Join;
```

If $\Delta E > 0$, extra energy is needed for implementing the join decision and, at this point, the energy stored in the tanks is exploited. First, the agents check if there is enough energy in their tanks to cover for ΔE (line 4). If this is the case, the amount of energy ΔE_{ij}

$$\Delta E_{ij} = \frac{T(t_i)}{T(t_i) + T(t_j)} \Delta E \tag{15}$$

is extracted from the tank of agent i by means of the input w_{ij}. At the same time agent j will extract ΔE_{ji} from its tank using w_{ji} Then, the join is safely implemented (line 9).

If the energy stored in the tanks of the two agents is not sufficient, there is still a chance to passively join the agents without intervening directly on the dynamics of the robots. In fact, it may happen that the tanks of the rest of the fleet, in average, contain enough energy. Thus (line 5), agent i asks the fleet to activate the β_i in order to switch to consensus mode[5]. Then, the consensus is run until the redistribution of the energy among the tanks is completed. Eventually, all the agents switch back to normal mode ($\beta_i = 0$): all the tanks will

[4]Formally speaking, the action of inputs w_{ij} and w_{ji} corresponds to moving the state of (9) from x^s_{ij} to the new actual inter-agent displacement $x_i - x_j$.

[5]This can be done by using a decentralized procedure (e.g., the classic flooding algorithm) so that all the agents belonging to the same connected component of the communication graph set $\beta_i = 1$.

contain the same amount of energy, but the total tank energy will remain unchanged. After this redistribution, agents i and j check again if there is enough energy in the tanks for joining (line 6). If this is the case, the tank of agent i is updated by means of the input w_{ij} in order to extract the amount of energy in (15) (and symmetrically on agent j), and the join decision is implemented (lines 8, 9). If, after all, the energy in the tanks is not yet sufficient, it is necessary to act directly on the robots to refill the tanks. This is always possible by augmenting the artificial damping on the agents for increasing the energy dissipation rate. The damping is augmented until $T(t_i) + T(t_j) \geq \Delta E + 2\epsilon$, so that the join decision can be passively implemented extracting the needed amount of energy through the input w_{ij} (lines 7, 8, 9).

Remark 5. *We assume the convergence time of the consensus to be fast enough compared to the dynamics of the fleet for joining the agents and re-establishing the desired behavior as quickly as possible. In fact, if the algorithm is too slow, the agents may come very close to each other without feeling any repulsive force. If the consensus is not fast enough and some dangerous situation is detected, it can be switched off for dampening the system in order to refill the tanks.*

Remark 6. *When the damping of the agents is augmented, some time may be needed to refill the tanks up to the desired energy value. During this period, agents i and j can still move because of the interaction with the rest of the group: in this case, their relative distance d_{ij} and the amount of energy necessary for implementing the join will change. Therefore, it is necessary to continuously update ΔE when the agents are in damping mode.*

The behavior of the slave side when the `PassiveJoin` Procedure is implemented can be described by the following system:

$$\begin{cases} \begin{pmatrix} \dot{p} \\ \dot{x} \\ \dot{t} \end{pmatrix} = \left[\begin{pmatrix} 0 & \mathcal{I}(t) & 0 \\ -\mathcal{I}^T(t) & 0 & \Gamma^T \\ 0 & -\Gamma & 0 \end{pmatrix} - \right. \\ \left. - \begin{pmatrix} B & 0 & 0 \\ 0 & 0 & 0 \\ -(I-\beta)\alpha PB & 0 & 0 \end{pmatrix} \right] \begin{pmatrix} \frac{\partial \mathcal{H}}{\partial p} \\ \frac{\partial \mathcal{H}}{\partial x} \\ \frac{\partial \mathcal{H}}{\partial t} \end{pmatrix} + \begin{pmatrix} 0 \\ 0 \\ \beta c \end{pmatrix} + GF^e \\ v = G^T \begin{pmatrix} \frac{\partial \mathcal{H}}{\partial p} \\ \frac{\partial \mathcal{H}}{\partial x} \\ \frac{\partial \mathcal{H}}{\partial t} \end{pmatrix} \end{cases} \tag{16}$$

where

$$\mathcal{H} = \sum_{i=1}^{N} \mathcal{K}_i + \sum_{i=1}^{N-1} \sum_{j=i+1}^{N} V(x_{ij}) + \sum_{i=1}^{N} T_i \tag{17}$$

is the augmented total energy of the system. The matrix $\Gamma \in \mathbb{R}^{N \times \frac{3N(N-1)}{2}}$ represents the interconnection among tanks and elastic elements mediated by inputs w_{ij}. From (8), one can readily verify that matrix Γ has a structure 'equivalent' to the incidence matrix $\mathcal{I}_\mathcal{G}$ with the $(i,\, j)$-th element being replaced by the (row) vector w_{ij}^T. Formally, by letting Γ_{ij} and $\mathcal{I}_{\mathcal{G}_{ij}}$ represent the $(i,\, j)$-th elements of Γ and $\mathcal{I}_\mathcal{G}$, respectively, it is

$$\Gamma_{i,(3j-2\ldots 3j)} = \mathcal{I}_{\mathcal{G}_{ij}} w_{ij}^T, \forall i = 1 \ldots N,\ \forall j = 1 \ldots N(N-1)/2.$$

Finally, $\alpha = diag(\alpha_i)$ and $\beta = diag(\beta_i)$ are matrices containing the mode switching parameters, $P = diag(\frac{1}{t_i} p_i^T M_i^{-T})$, $t = (t_1, \ldots, t_N)^T$, and $c = (c_1, \ldots, c_N)^T$.

Proposition 3. *The system represented in* (16) *is passive w.r.t. the input/output pair* $(F^e,\, v)$ *with storage function* $\mathcal{H}$.

Proof: By evaluating the time derivative of the storage function

$$\dot{\mathcal{H}} = \begin{pmatrix} \frac{\partial^T \mathcal{H}}{\partial p} & \frac{\partial^T \mathcal{H}}{\partial x} & \frac{\partial^T \mathcal{H}}{\partial t} \end{pmatrix} \begin{pmatrix} \dot{p} \\ \dot{x} \\ \dot{t} \end{pmatrix} \tag{18}$$

along the system trajectories, we obtain:

$$\dot{\mathcal{H}} = -\frac{\partial^T \mathcal{H}}{\partial p} B \frac{\partial \mathcal{H}}{\partial p} + \frac{\partial^T \mathcal{H}}{\partial t} (I-\beta)\alpha PB \frac{\partial \mathcal{H}}{\partial p} + \beta \frac{\partial \mathcal{H}}{\partial t} c + v^T F^e = h_1 + h_2 + h_3 + v^T F^e \tag{19}$$

The system is passive if the sum of the first three terms of (19) is lower or equal than 0. The first term h_1 is always non positive because B is positive definite. The parameter β can either be equal to the null or identity matrix.

When $\beta = 0$, $h_3 = 0$ and the second term

$$h_2 = \frac{\partial^T \mathcal{H}}{\partial t} \alpha PB \frac{\partial \mathcal{H}}{\partial p} = \begin{pmatrix} t_1 \ldots t_N \end{pmatrix} \alpha \begin{pmatrix} \frac{1}{t_1} D_1 \\ \vdots \\ \frac{1}{t_N} D_N \end{pmatrix} = \sum_{i=1}^{N} \alpha_i D_i \tag{20}$$

is, because of (12), at most equal to the energy dissipated by the agents, i.e, $-h_1$. Therefore, $\dot{\mathcal{H}} \leq v^T F^e$.

When $\beta = I$, $h_2 = 0$ and the consensus is running among the tanks. By recalling (14), h_3 can be written as

$$h_3 = \frac{\partial^T \mathcal{H}}{\partial t} c = \sum_{i=1}^{N} \dot{T}_i. \tag{21}$$

Because of the property of the consensus, the overall energy stored in the tanks remains the same and, therefore, $h_3 = 0$ and $\dot{\mathcal{H}} \leq v^T F^e$. ∎

Remark 7. *Note that, although (16) has a switching dynamics because of the time-varying nature of $\mathcal{I}(t)$ arising from the neighboring conditions $\sigma_{ij}(t)$ of Def. 1, stability issues are avoided thanks to the action of the* `PassiveJoin` *Procedure which prevents positive jumps in $\mathcal{H}$ at any switching time.*

B. The Master Side

The master can be a generic mechanical system modeled by the following Euler-Lagrange equations:

$$M_M(x_M)\ddot{x}_M + C_M(x_M, \dot{x}_M)\dot{x}_M + D_M \dot{x}_M = F_M \tag{22}$$

where x_M and $\dot{x}_M$ represent the position and the velocity of the end-effector, $M_M(x_M)$ represents the inertia matrix, $C(x_M, \dot{x}_M)\dot{x}_M$ is a term representing the centrifugal and Coriolis effects, D_M is matrix representing both the viscous friction present in the system and any additional damping injection via local control actions. As often happens for master devices, we also assume that gravity effects are locally compensated. A system described by (22) is passive with respect

to the force-velocity pair (F_M, v_M) [33], where $v_M := \dot{x}_M$. This kind of passivity is well suited in standard passivity-based bilateral teleoperation, where the velocity of the master and the velocity of the slave need to be synchronized.

Nevertheless, in our setting, in order to consider the difference between the workspace of the master and that of the robots at the slave side, it is necessary to synchronize the *position* of the master with the *velocity* of the leader. Unfortunately, a mechanical system is not passive w.r.t. the position-force pair but, following [34], it is possible to render the master (22) passive w.r.t. the pair (F_M, r) with storage function $V_M = \frac{1}{2} r^T M_M r$ and $r = v_M + \lambda x_M$, $\lambda > 0$. This is obtained by a suitable pre-feedback action requiring knowledge of the matrixes M_M and C_M in (22). By further introducing a scaling into this strategy, one can also render the master passive w.r.t. the scaled pair (F_M, r_M) where

$$r_M = \rho r = \rho v_M + \rho\lambda x_M = \rho v_M + K x_M, \qquad (23)$$

$\rho > 0$, $\lambda > 0$, and new (scaled) storage function $\bar{V}_M = \rho V_M$. The following result then easily follows:

Proposition 4. *A mechanical system which has been made passive with respect to the pair (r, F_M) is also passive with respect to the pair (r_M, F_M)*

Proof: Since the system is passive with respect to the pair (r, F_M) it is

$$r^T F_M \geq \dot{V}_M \qquad (24)$$

Using (23), we have that

$$r_M^T F_M = \rho r^T F_M \geq \rho \dot{V}_M = \dot{\bar{V}}_M. \qquad (25)$$

Therefore, the system is passive w.r.t the lower bounded function $\bar{V}_M$. ■

Thus, by properly choosing ρ and λ it is possible to make negligible the contribution related to $\dot{x}_M$ (by choosing a small ρ), and make the second term proportional to the position with a desired scaling factor K (by choosing $\lambda = \frac{K}{\rho}$)

C. Master-slave Interconnection

Exploiting the results developed so far, we have that both master and slave sides are passive systems. Thus, by designing a proper passive interconnection between the local and the remote systems, we will obtain a passive bilateral teleoperation system characterized by a stable behavior in case of interaction with passive environments (as the obstacles, modeled as potentials, with which the fleet is interacting).

Suppose that agent l is chosen as the leader. It is possible to write $F_l^e = F_s + F_l^{\text{env}}$, where F_l^{env} is the component of the force due to the interaction with the external environment (obstacles) and F_s is the component due to the interaction with the master side. Similarly, we can decompose F_M as $F_M = F_m + F_h$, where F_h is the component due to the interaction with the user and F_m is the force acting on the master because of the interaction with the slave.

For achieving the desired teleoperation behavior, we propose to join master and slave using the following interconnection:

$$\begin{cases} F_s = b_T(r_M - v_l) \\ F_m = -b_T(r_M - v_l) \end{cases}, \quad b_T > 0 \qquad (26)$$

This is equivalent to joining the master and the leader using a damper which generates a force proportional to the difference of the two velocity-like variables of the master and the leader. Since r_M is "almost" the position of the master, we have that the force fed back to the master and the control action sent to the leader are the desired ones. The overall teleoperation system is represented in Fig. 1 and consists of the interconnection of a passive master side, a damper-like interconnection and a passive slave side. By letting $\bar{F}^e = \begin{pmatrix} F_1^{e^T} & \cdots & F_l^{env^T} & \cdots & F_N^{e^T} \end{pmatrix}^T$ be the vector of the forces due to the interaction with the external environment, the following Proposition holds:

Proposition 5. *The teleoperation system composed by the precompensated master side presented in Sec. II-B, the slave side reported in* (16)*, and the interconnection* (26) *is passive with respect to the pair $((\bar{F}^e)^T, F_h^T)^T, (v^T, r_M^T)^T$.*

Proof: Considering the decomposition of F_M and of F_l^e, from Proposition 3 and from (25) we can state that

$$\begin{cases} v^T F^e = v^T \bar{F}^e + v_l^T F_s \geq \dot{\mathcal{H}} \\ r_M^T F_h + r_M^T F_m \geq \dot{\bar{V}}_M \end{cases} \qquad (27)$$

Since (26) implies

$$v_l^T F_s + r_M^T F_m = -b_T (r_M - v_l)^T (r_M - v_l) \leq 0, \qquad (28)$$

by taking $\mathcal{H}_{tot} = \mathcal{H} + \bar{V}_M$ as lower bounded storage function, and by exploiting (27) and (28), it follows that

$$v^T \bar{F}^e + r_M^T F_h \geq \dot{\mathcal{H}}_{tot} + b_T (r_M - v_l)^T (r_M - v_l) \geq \dot{\mathcal{H}}_{tot}. \qquad (29)$$

This proves passivity of the master/slave interconnection. ■

It is also straightforward to passively consider communication delays between local and remote sites using one of the techniques developed for single-master single-slave systems, like, for example, the two-layer approach [35]. In this way, the system would keep on exhibiting a stable behavior independently of any delay between local and remote sites[6].

III. Steady-State Analysis

Without loss of generality we assume in this Section that agent $l = 1$ is the leader, implying that $F_1^e = F_1^{\text{env}} + F_s$ and $F_i^e = F_i^{\text{env}}$ for $i = 2 \dots N$. The goal of the following analysis is to characterize the steady-state behavior of the overall teleoperation system in two relevant regimes: free-motion (i.e., $F_i^{\text{env}} = 0$, $\forall i = 1, \dots, N$), and hard contact with obstacles (i.e., $v_i = 0$, $\forall i = 1, \dots, N$, despite $r_M \neq 0$).

A. Steady-state during free motion

We first consider the free-motion case and denote with $\mathcal{G}_{\mathcal{L}}$ the connected component of $\mathcal{G}$ containing the leader. In this situation, we assume that (i) the agents are sufficiently far away from any obstacle so that $F_i^{\text{env}} = 0$, $\forall i$, (ii) there exists a certain time $\bar{\tau}$ after which no splits and joins take place in $\mathcal{G}_{\mathcal{L}}$ and tanks are fully charged at their maximum value

[6]We assume that negligible delays are present within the slave-side because of the spatial proximity of the agents.

$\bar{T}_i$, and (iii) the master device is kept at a constant position $\bar{x}_M \equiv const$ by a suitable human force F_h whose steady-state value will be determined in the following.

The following Proposition shows that, under these assumptions, the robots belonging to $\mathcal{G}_\mathcal{L}$ reach a steady-state regime in which all the agents possess the same velocity $v_{ss} \in \mathbb{R}^3$ as a function of $\bar{x}_M$. In addition, it also indicates the steady-state value of the force F_h exerted by the human operator to keep the master device at $\bar{x}_M$. We start introducing the following preliminary definitions: we assume that $\mathcal{G}_\mathcal{L}$ contains $1 \leq N_\mathcal{L} \leq N$ agents whose indexes are collected into the set $\mathcal{L}$, so that $|\mathcal{L}| = N_\mathcal{L}$. Note that $1 \in \mathcal{L}$ by construction. We then let $p_\mathcal{L} \in \mathbb{R}^{3N_\mathcal{L}}$, $x_\mathcal{L} \in \mathbb{R}^{\frac{3N_\mathcal{L}(N_\mathcal{L}-1)}{2}}$, $t_\mathcal{L} \in \mathbb{R}^{N_\mathcal{L}}$ represent the entries of p, x and t associated to this component, and $p_{\bar{\mathcal{L}}} \in \mathbb{R}^{3(N-N_\mathcal{L})}$, $x_{\bar{\mathcal{L}}} \in \mathbb{R}^{\frac{3(N-N_\mathcal{L})(N-N_\mathcal{L}-1)}{2}}$ and $t_{\bar{\mathcal{L}}} \in \mathbb{R}^{N-N_\mathcal{L}}$ the remaining ones, where $\bar{\mathcal{L}}$ denotes the complement of $\mathcal{L}$. Accordingly, we let $\mathcal{H}_\mathcal{L}$ and $\mathcal{H}_{\bar{\mathcal{L}}}$ be the components of the total energy $\mathcal{H}$ depending on $(p_\mathcal{L}, x_\mathcal{L}, t_\mathcal{L})$ and $(p_{\bar{\mathcal{L}}}, x_{\bar{\mathcal{L}}}, t_{\bar{\mathcal{L}}})$, respectively. Furthermore, we let $\mathbf{1}_{N_{\mathcal{L}3}} = \mathbf{1}_{N_\mathcal{L}} \otimes I_3$ with $\mathbf{1}_{N_\mathcal{L}} \in \mathbb{R}^{N_\mathcal{L}}$ being a column vector of all ones, and $B_\mathcal{L} \in \mathbb{R}^{3N_\mathcal{L} \times 3N_\mathcal{L}} = diag(B_{\mathcal{L}_i})$, with $B_{\mathcal{L}_1} = B_1 + b_T I_3$ and $B_{\mathcal{L}_i} = B_i$, $i \in \mathcal{L}$, $i \neq 1$. Finally, we define with v_{ss} and F_{ss} the (sought) steady-state values for the agents in $\mathcal{L}$ and for the force exerted by the human operator.

Proposition 6 (Steady-state in free motion)**.** *Under assumptions (i), (ii), and (iii), the system* (16) *reaches a steady-state characterized by $(\dot{p}, \dot{x}, \dot{t}) = (0, 0, 0)$ in which:*

1) *every robot belonging to $\bar{\mathcal{L}}$ comes to a full stop;*
2) *every robot belonging to $\mathcal{L}$ has the same velocity $v_{ss} = (\mathbf{1}_{N_{\mathcal{L}3}}^T B_\mathcal{L} \mathbf{1}_{N_{\mathcal{L}3}})^{-1} b_T K \bar{x}_m$;*
3) *the human operator needs to apply a force $F_h = (I_3 - b_T(\mathbf{1}_{N_{\mathcal{L}3}}^T B_\mathcal{L} \mathbf{1}_{N_{\mathcal{L}3}})^{-1}) b_T K \bar{x}_m$ to keep the master device at $\bar{x}_M$.*

Proof: We start by noting that, $\forall$ x_{ij} not included in $x_\mathcal{L}$ and $x_{\bar{\mathcal{L}}}$, $\dot{x}_{ij} = 0$ as it necessarily represents the state of a disconnected virtual spring. Furthermore, the subsystem $(p_{\bar{\mathcal{L}}}, x_{\bar{\mathcal{L}}}, t_{\bar{\mathcal{L}}})$ not belonging to $\mathcal{L}$ is governed by the dynamics

$$\begin{pmatrix} \dot{p}_{\bar{\mathcal{L}}} \\ \dot{x}_{\bar{\mathcal{L}}} \\ \dot{t}_{\bar{\mathcal{L}}} \end{pmatrix} = \begin{pmatrix} -B_{\bar{\mathcal{L}}} & \mathcal{I}_{\bar{\mathcal{L}}} & 0 \\ -\mathcal{I}_{\bar{\mathcal{L}}}^T & 0 & 0 \\ 0 & 0 & 0 \end{pmatrix} \begin{pmatrix} \frac{\partial \mathcal{H}_{\bar{\mathcal{L}}}}{\partial p_{\bar{\mathcal{L}}}} \\ \frac{\partial \mathcal{H}_{\bar{\mathcal{L}}}}{\partial x_{\bar{\mathcal{L}}}} \\ \frac{\partial \mathcal{H}_{\bar{\mathcal{L}}}}{\partial t_{\bar{\mathcal{L}}}} \end{pmatrix} \tag{30}$$

for some $\mathcal{I}_{\bar{\mathcal{L}}}$ and positive definite $B_{\bar{\mathcal{L}}}$ of proper dimensions. Since the tanks are supposed to be full (Assumption (ii)), no energy exchange takes place among tanks and elastic elements, and $\dot{t}_{\bar{\mathcal{L}}} = 0$. Therefore, by evaluating the rate of change of $\mathcal{H}_{\bar{\mathcal{L}}}$ along (30), one obtains

$$\dot{\mathcal{H}}_{\bar{\mathcal{L}}} = -\frac{\partial^T \mathcal{H}_{\bar{\mathcal{L}}}}{\partial p_{\bar{\mathcal{L}}}} B_{\bar{\mathcal{L}}} \frac{\partial \mathcal{H}_{\bar{\mathcal{L}}}}{\partial p_{\bar{\mathcal{L}}}} \leq 0,$$

that is, the system is output strictly passive, implying that the system will converge towards the condition $\frac{\partial \mathcal{H}_{\bar{\mathcal{L}}}}{\partial p_{\bar{\mathcal{L}}}} = v_{\bar{\mathcal{L}}} \equiv 0 \Rightarrow p_{\bar{\mathcal{L}}} \equiv 0 \Rightarrow \dot{p}_{\bar{\mathcal{L}}} \equiv 0$. From the second row of (30), this further implies that $\dot{x}_{\bar{\mathcal{L}}} \equiv 0$, resulting in a steady-state $(\dot{p}_{\bar{\mathcal{L}}}, \dot{x}_{\bar{\mathcal{L}}}, \dot{t}_{\bar{\mathcal{L}}}) = (0, 0, 0)$ where all the agents in $\bar{\mathcal{L}}$ eventually reach a full stop ($v_{\bar{\mathcal{L}}} = 0$). This proves item 1) of the Proposition.

Coming to items 2) and 3), note that, because of assumption (iii), we have $\dot{x}_M = \ddot{x}_M \equiv 0$ and $r_M = K\bar{x}_M$. By splitting F_s into the two components $b_T K \bar{x}_M$ and $-b_T v_1$, the subsystem $(p_\mathcal{L}, x_\mathcal{L}, t_\mathcal{L})$ belonging to $\mathcal{L}$ becomes

$$\begin{cases} \begin{pmatrix} \dot{p}_\mathcal{L} \\ \dot{x}_\mathcal{L} \\ \dot{t}_\mathcal{L} \end{pmatrix} = \begin{pmatrix} -B_\mathcal{L} & \mathcal{I}_\mathcal{L} & 0 \\ -\mathcal{I}_\mathcal{L}^T & 0 & 0 \\ 0 & 0 & 0 \end{pmatrix} \begin{pmatrix} \frac{\partial \mathcal{H}_\mathcal{L}}{\partial p_\mathcal{L}} \\ \frac{\partial \mathcal{H}_\mathcal{L}}{\partial x_\mathcal{L}} \\ \frac{\partial \mathcal{H}_\mathcal{L}}{\partial t_\mathcal{L}} \end{pmatrix} + \begin{pmatrix} u \\ 0 \end{pmatrix} \\ v_\mathcal{L} = G^T \begin{pmatrix} \frac{\partial \mathcal{H}_\mathcal{L}}{\partial p_\mathcal{L}} \\ \frac{\partial \mathcal{H}_\mathcal{L}}{\partial x_\mathcal{L}} \\ \frac{\partial \mathcal{H}_\mathcal{L}}{\partial t_\mathcal{L}} \end{pmatrix} \end{cases} \tag{31}$$

where $\mathcal{I}_\mathcal{L} = (\mathcal{I}_{\mathcal{G}_\mathcal{L}} \otimes I_3)$, $\mathcal{I}_{\mathcal{G}_\mathcal{L}}$ being the incidence matrix associated to $\mathcal{G}_\mathcal{L}$, and $u \in \mathbb{R}^{3N_\mathcal{L}}$ is a constant vector whose first 3 entries are $b_T K \bar{x}_M$ and the remaining ones are zero. In order to draw conclusions on the asymptotical (steady-state) behavior of (31) when excited with a constant u, we resort to the arguments illustrated in Proposition 8.1.1 of [36]. To this end, consider the constant input u as being generated by the following neutrally stable exosystem

$$\begin{cases} \dot{\omega} = 0 \\ u = \omega \end{cases}. \tag{32}$$

Note also that, since system (31) is again output strictly passive, when $u = 0$ one obtains

$$\dot{\mathcal{H}}_\mathcal{L} = -\frac{\partial^T \mathcal{H}_\mathcal{L}}{\partial p_\mathcal{L}} B_\mathcal{L} \frac{\partial \mathcal{H}_\mathcal{L}}{\partial p_\mathcal{L}} \leq 0,$$

yielding an asymptotically stable equilibrium point corresponding to a (local) minimum of its energy. Therefore, the assumptions required by Proposition 8.1.1 are met and system (31) admits a steady-state regime. This is characterized by a map $\pi(\cdot)$

$$\pi : \omega \mapsto \begin{pmatrix} p_\mathcal{L} \\ x_\mathcal{L} \end{pmatrix}, \quad \pi(\omega) = \begin{pmatrix} \pi_1(\omega) \\ \pi_2(\omega) \end{pmatrix} \tag{33}$$

satisfying the following condition

$$0 = \begin{pmatrix} -B_\mathcal{L} & \mathcal{I}_\mathcal{L} \\ -\mathcal{I}_\mathcal{L}^T & 0 \end{pmatrix} \begin{pmatrix} M_\mathcal{L}^{-1} \pi_1(\omega) \\ \nu(\pi_2(\omega)) \end{pmatrix} + \begin{pmatrix} \omega \\ 0 \end{pmatrix} \tag{34}$$

where $\nu(\cdot) := \frac{\partial \mathcal{H}}{\partial x}(\cdot)$ and $M_\mathcal{L}$ is the inertia matrix associated to the agents in $\mathcal{L}$. Now, rewrite (34) as

$$B_\mathcal{L} M_\mathcal{L}^{-1} \pi_1(\omega) - \mathcal{I}_\mathcal{L} \nu(\pi_2(\omega)) = \omega \tag{35}$$

$$\mathcal{I}_\mathcal{L}^T M_\mathcal{L}^{-1} \pi_1(\omega) = 0. \tag{36}$$

As the group of agents that we are considering is connected, it is well known that $\mathrm{rank}(\mathcal{I}_{\mathcal{G}_\mathcal{L}}^T) = N_\mathcal{L} - 1$ and $\ker(\mathcal{I}_{\mathcal{G}_\mathcal{L}}^T) = \mathbf{1}_{N_\mathcal{L}}$, see, e.g., [19]. Then from (36) it follows that

$$M_\mathcal{L}^{-1} \pi_1(\omega) = \mathbf{1}_{N_{\mathcal{L}3}} v_{ss}, \tag{37}$$

for a certain $v_{ss} \in \mathbb{R}^3$. Plugging (37) into (35), we obtain

$$\mathcal{I}_\mathcal{L} \nu(\pi_2(\omega)) = B_\mathcal{L} \mathbf{1}_{N_{\mathcal{L}3}} v_{ss} - \omega. \tag{38}$$

This is a linear equation in the unknowns $\nu(\pi_2(\omega))$ and it admits a solution iff the rhs belongs to $\mathrm{Im}(\mathcal{I}_\mathcal{L})$. Since, from standard linear algebra, $\mathrm{Im}(\mathcal{I}_\mathcal{L}) = \ker(\mathcal{I}_\mathcal{L}^T)^\perp = \mathrm{span}(\mathbf{1}_{N_{\mathcal{L}3}})^\perp$, the rhs of (38) must satisfy

$$\mathbf{1}_{N_{\mathcal{L}3}}^T (B_\mathcal{L} \mathbf{1}_{N_{\mathcal{L}3}} v_{ss} - \omega) = 0.$$

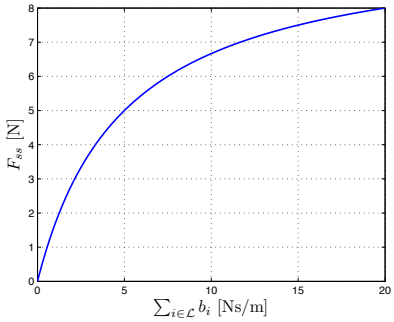

Fig. 4: The steady-state force F_{ss} during free-motion as a function of the total damping of the agents belonging to $\mathcal{L}$. Note how F_{ss} increases with the number of agents $N_{\mathcal{L}}$ belonging to $\mathcal{L}$.

This condition yields the sought value for the steady-state agent velocities

$$v_{ss} = (\mathbf{1}_{N_{\mathcal{L}3}}^T B_{\mathcal{L}} \mathbf{1}_{N_{\mathcal{L}3}})^{-1} \mathbf{1}_{N_{\mathcal{L}3}}^T \omega = (\mathbf{1}_{N_{\mathcal{L}3}}^T B_{\mathcal{L}} \mathbf{1}_{N_{\mathcal{L}3}})^{-1} b_T K \bar{x}_M. \tag{39}$$

Therefore, by taking v_{ss} as in (39), it is always possible to solve (38) for some $\nu(\pi_2(\omega))$ whose specific value is, however, not required for this analysis. Thus, the steady-state for system (31) is given by:

$$\begin{pmatrix} p_{\mathcal{L}ss} \\ x_{\mathcal{L}ss} \end{pmatrix} := \pi(\omega) = \begin{pmatrix} M_{\mathcal{L}} \mathbf{1}_{N_{\mathcal{L}3}} v_{ss} \\ \nu(\pi_2(\omega)) \end{pmatrix} = const \tag{40}$$

as $\omega = const$ by definition. Furthermore, expanding (40), for each agent $i \in \mathcal{L}$ at steady-state it is $v_i = M_i^{-1} p_i = M_i^{-1} M_i v_{ss} = v_{ss}$, that is, all the agents in $\mathcal{L}$ will reach the same steady-state velocity v_{ss}, proving item 2).

Finally, noting that (22) and the assumption (iii) $\ddot{x}_M = \dot{x}_M = 0$ imply $0 = F_M = F_m + F_h$, we have, at steady-state

$$\begin{aligned} F_h = -F_m = F_{ss} := b_T(K\bar{x}_M - v_{ss}) = \\ = (I_3 - b_T(\mathbf{1}_{N_{\mathcal{L}3}}^T B_{\mathcal{L}} \mathbf{1}_{N_{\mathcal{L}3}})^{-1}) b_T K \bar{x}_M \end{aligned} \tag{41}$$

which proves item 3) and concludes the proof. ■

Remark 8. *Note that* (39) *is always well-posed because $B_{\mathcal{L}}$ is a positive definite matrix. In the particular case of damping terms taking the form $B_i = b_i I_3$, $b_i > 0$,* (39) *reduces to*

$$v_{ss} = \frac{b_T K \bar{x}_M}{b_T + \sum_{i\in\mathcal{L}} b_i} \tag{42}$$

and (41) *becomes*

$$F_{ss} = \frac{b_T K \bar{x}_M \sum_{i\in\mathcal{L}} b_i}{b_T + \sum_{i\in\mathcal{L}} b_i} \tag{43}$$

It is easy to check that, as $\left(\sum_{i\in\mathcal{L}} b_i\right)/b_T \to 0$ (small b_i, large b_T), $v_{ss} \to K\bar{x}_M = r_M$ and $F_{ss} \to 0$, thus approaching perfect synchronization with the commanded velocity r_M. The same, however, holds also for the more general forms (39) and (41).

At steady-state, the human operator needs to apply a force $F_h = F_{ss}$ proportional to the commanded velocity $K\bar{x}_M$ by a factor which depends on the number of agents $N_{\mathcal{L}}$ belonging to the connected component of the leader $\mathcal{L}$, and on the magnitude of their damping terms in B_i. For a given $\mathcal{L}$, force F_h will mimic a spring centered on a zero velocity command (see (41)–(43)). Thus, if the number of agents in $\mathcal{L}$ is constant, this force cue will increase/decrease proportionally to the steady-state absolute speed of the whole group: this can provide an haptic cue informative of the overall group velocity.

On the other hand, for a given *fixed* commanded velocity $K\bar{x}_M$, F_h will still vary with the size of $\mathcal{L}$ because of the term $\sum_{i\in\mathcal{L}} b_i$ in (43). Figure 4 shows an illustrative behavior of F_h in this case with $\bar{x}_M \equiv 2$, $K = 1$, and $b_T = 5$. One can then check that the force F_h needed to keep a constant velocity $K\bar{x}_M$ increases with the size of $N_{\mathcal{L}}$. This behavior can also be intuitively explained by considering the followers as a passive environment the leader is interacting with. In fact, it is known from standard bilateral teleoperation (see, e.g., [37]) that in this case perfect steady-state 'synchronization' between master and slave velocities cannot be achieved resulting in a residual non-null steady-state force.

However, we believe that this behavior can constitute a beneficial feature of our teleoperation design. In fact, the force F_h resulting from such master/slave velocity mismatch can provide the user with an additional information about the status of the group. Consider the illustrative example where the operator is moving the whole fleet with a constant cruise speed by firmly keeping the master device at a certain constant position $\bar{x}_M$. By virtue of (41), whenever a robot disconnects from the group $\mathcal{L}$ the human operator would feel a decrease in the force needed to keep the master device at x_M. This negative slope in F_h can be informative of the fact that the number of robots in the connected component of leader has decreased. Similarly, when a robot connects to the group, the user would feel a positive slope in F_h, thus informing him/her about the increased number of robots in $\mathcal{L}$.

B. Steady-state during hard contact with obstacles

We now proceed to analyze the hard contact situation corresponding to the case where, in addition to assumptions (ii) and (iii), we also assume that (iv) $\frac{\partial \mathcal{H}_{\mathcal{L}}}{\partial p_{\mathcal{L}}} =: v_{\mathcal{L}} \equiv 0$ despite $r_M \neq 0$ (e.g., because the obstacles are obstructing the agent motion).

Proposition 7 (Hard contact with obstacles)**.** *Under the assumptions (ii), (iii) and (iv), the system* (16) *reaches a steady-state characterized by $(\dot{p}, \dot{x}, \dot{t}) = (0, 0, 0)$ in which:*

1) *every robot belonging to $\bar{\mathcal{L}}$ comes to a full stop;*
2) *there is a perfect force reflection on the human operator of the cumulative environmental forces stopping the robots belonging to $\mathcal{L}$, that is $F_h = -\sum_{i\in\mathcal{L}} F_i^{env}$.*

Proof: Proof of Item 1) follows from the same arguments used in Prop. 6. Because of assumption (iv) ($v_{\mathcal{L}} = 0$), the first row of (31) reduces to

$$0 = \mathcal{I}_{\mathcal{L}} \frac{\partial \mathcal{H}_{\mathcal{L}}}{\partial x_{\mathcal{L}}} + u, \tag{44}$$

where now $u \in \mathbb{R}^{3N_{\mathcal{L}}} = (\dots\, u_i^T\, \dots)$, $i \in \mathcal{L}$, with $u_1 = F_s + F_1^{\text{env}}$ and $u_i = F_i^{\text{env}}$, $i \neq 1$. By left-multiplying (44) with $\mathbf{1}_{N_{\mathcal{L}3}}^T$, and by exploiting again the fact that $\ker(\mathcal{I}_{\mathcal{L}}) = \text{span}(\mathbf{1}_{N_{\mathcal{L}3}})$, we get $\mathbf{1}_{N_{\mathcal{L}3}}^T u = 0$ that can be expanded as $F_s =$

$-\sum_{i\in\mathcal{L}} F_i^{\text{env}}$. Furthermore, because of assumption (iii), it is again $0 = F_M = F_h + F_m$ and, by using (26), we finally obtain

$$F_h = -F_m = F_s = -\sum_{i\in\mathcal{L}} F_i^{\text{env}}.$$

This proves Item 2) and concludes the proof. ■

IV. Simulation and Experimental Results

In this Section, we will report the results of several human/hardware-in-the-loop (HHL) simulations and experiments conducted to validate the theoretical framework developed so far. A picture representing our testbed is shown in Fig 5. The master side consists of a 3-DOF force-feedback device, the Omega.3[7] (Fig. 5c), controlled via usb by a C++ program running on a dedicated GNU-Linux machine. This includes two threads: the first thread runs a synchronous loop at 2.5 KHz which accesses the current master position/velocity and sets the control force F_m in (26). The second thread, running at a slower rate triggered by the leader control rate (60 Hz in the simulation case and 120 Hz for the experiments), acts as a network interface with the leader agent by exchanging the leader speed v_l and the master command r_M. By using the standard interface provided by the manufacturer, we are able to apply a 3-dimensional Cartesian force to the end-effector and to automatically compensate for gravity terms.

In order to illustrate the flexibility of our method, we conducted several HHL simulations with a slave side consisting of a heterogeneous group of robots including both quadrotor UAVs and differentially-driven ground robots (UGVs). All the robots are physically simulated within a custom-made environment based on the Ogre3D engine for 3D rendering and computational geometry caculations, and PhysX for simulating the physical interaction between the mobile robots and the environment[8] (see Figs. 5a,b,d). Note that both class of mobile robots meet the assumption of Remark 1. In particular, we relied on a cascaded controller for the UAV cartesian motion and on a PID controller for the attitude (i.e., pitch and roll) and yaw-rate DOFs. As for the UGVs, we employed a standard trajectory controller based on feedback linearization. Each mobile-robot (UAV/UGV) trajectory controller runs, in a decentralized way, as a separate process. This design facilitates the porting of the whole implementation on real hardware. Every process is in charge of (1) communicating with the other mobile robots, (2) communicating with the master device (only the process controlling the leader), (3) implementing the inter-agent behavior described in Sec. II-A, (4) retrieving the current UAV/UGV state and the surrounding obstacle points from the simulator, and (5) implementing the trajectory tracking controller mentioned in Remark 1. All the communication is implemented with the UDP protocol since it is less prone to congestions and delay issues compared to the TCP protocol.

In the experiments, the slave side is composed of 4 quadrotors[9] equipped with an embedded ATmega microcontroller and a standard integrated IMU (Fig. 5e). The microcontroller

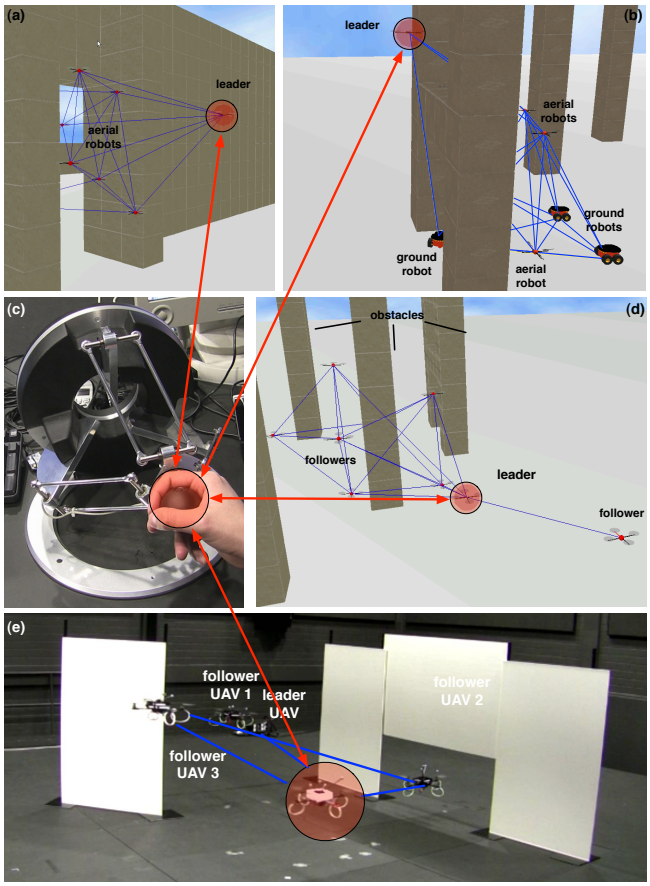

Fig. 5: The Human/Hardware-in-the-Loop simulative and experimental setup. Fig. 5(c): The Omega-3 force-feedback master device handled by the human operator. Figs. 5(a,b,d): 3 screenshots of a physically-based simulation in a cluttered environment involving a fleet of either 8 quadrotors (a,d), or 5 quadrotors and 3 differentially-driven ground robots (b). The leader is highlighted by a transparent red ball; inter-agent visibility and distance are considered as neighboring criteria; neighbor agents are linked by blue lines. Fig. 5(e): a screenshot of an experiment with 4 real quadrotors in a cluttered environment where the leader is highlighted by a transparent red ball.

implements a low-level PID attitude controller by estimating the current attitude from the IMU measurements (via a complementary filter), and by controlling the pitch, roll, thrust and yaw-rate dofs of the UAV. This PID controller runs at about 450 Hz. Every quadrotor is also equipped with an additional Qseven single-board GNU-Linux machine running a C++ program which implements a higher-level cartesian-control module: this computes the desired attitude and thrust commands and sends them to the low-level microprocessor via a serial interface whose baud rate is set to 115200. As opposite to the simulation case, the Qseven board (1) retrieves the current UAV position (and numerically estimates its velocity) from an external tracking system, and (2) receives the obstacle positions form the simulation environment where the physical obstacles are simulated in parallel. All the ethernet communication is again implemented with the UDP protocol.

In all simulations and experiments, we simulated the presence of a visibility sensor for retrieving the position of neighboring agents. Therefore, compatibly with the requirements of

[7] http://www.forcedimension.com
[8] http://www.ogre3d.org/, http://www.nvidia.com/object/physx_new.html
[9] http://www.mikrokopter.com

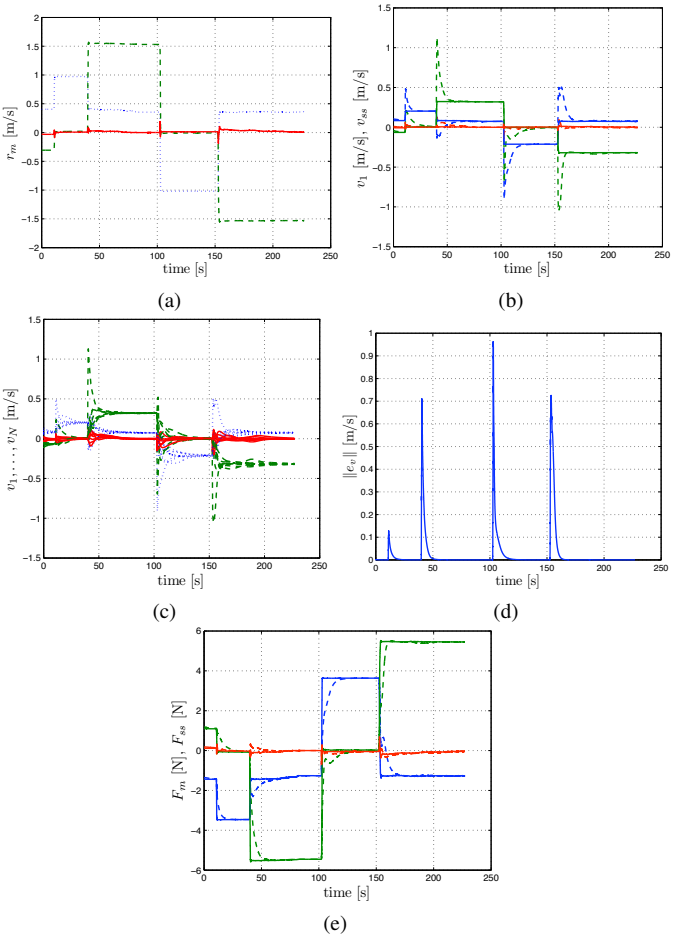

Fig. 6: Results of the first HHL simulation: a): velocity command $r_M(t)$ set by the human operator (three components, x solid blue, y dashed green, z dotted red); b) superimposition of $v_1(t)$ (the leader velocity in dashed lines) and $v_{ss}(t)$ (the predicted steady-state velocity in solid lines); c) superimposition of the velocities of all the agents (three components, x solid blue, y dashed green, z dotted red); d) behavior of $\|e_v\|$, the norm of the velocity error of every agent w.r.t. the predicted v_{ss}; e) superimposition of the force $F_m(t)$ applied to the master because of the interaction with the slave (dashed lines) and its predicted steady-state value F_{ss} (solid lines).

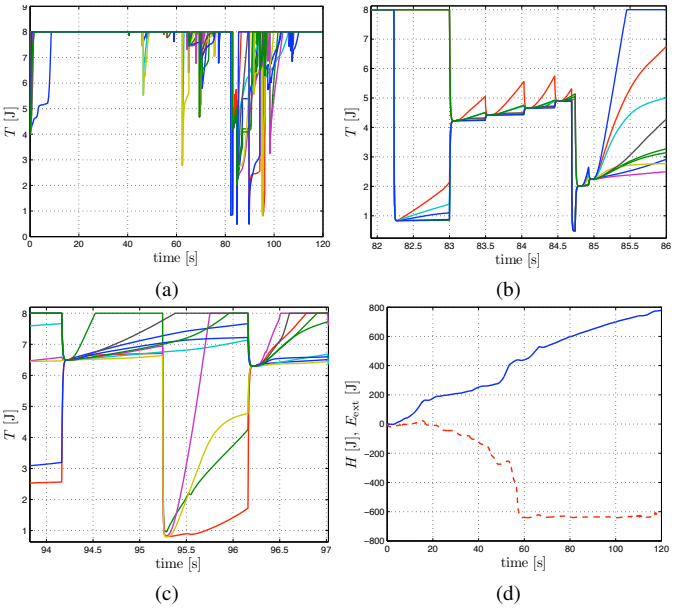

Fig. 7: Results of the second HHL simulation: a); behavior of $T(t)$ over time during several split and join decisions. Negative jumps in $T(t)$ correspond to energy exchanges between tanks and link potentials in order to ensure passivity of the slave-side (`PassiveJoin` Procedure); b-c) zoomed view of the tank energies during consecutive consensus phases; d) behavior of $E_{\text{ext}}(t)$ (blue line) $E_{\text{in}}(t)$ (red line), validating the slave side passivity condition (19) also during the split/join decisions.

Def. 1, we also set $\sigma_{ij} = 0$ whenever the line of sight between agents i and j was occluded. The agents were then forced to split either because of too large interdistances ($d_{ij} > D$), or because of occlusions on their line of sights, an event which can also occur when $d_{ij} < D$. Of course, different choices for deciding splits are possible, but they are equivalent w.r.t. the conceptual behavior of the `PassiveJoin` Procedure. We also assumed w.l.o.g. that the leader is agent 1. The reader is encouraged to watch the video clip attached to the paper where both simulations and experiments in cluttered environments with frequent split and join decisions can be fully appreciated.

A. Simulation Results

In the first HHL simulation, reported in Figs. 6(a–e), we tested the overall performance of the teleoperation scheme during free-motion (i.e., sufficiently away from obstacles). The goal was to validate the claims of Prop. 6 about stability and steady-state characteristics of our teleoperation system. We considered a leader and 7 followers, and teleoperated the leader with (almost) piece-wise constant velocity commands r_M, as shown in Fig. 6(a). During the simulation, we kept all the 7 agents within the connected component containing the leader $\mathcal{L}$, and chose $b_T = 4.5$ [Ns/m], $B_1 = 1I_3$ [Ns/m], $B_i = 2.3I_3$ [Ns/m] for $i = 2 \dots 8$, and $K = 15$ [1/s].

Figure 6(b) shows the superimposition of the actual leader velocity v_1 (dashed lines) and the predicted steady-state velocity v_{ss} (solid lines): as clear from the plot, when r_M is kept constant v_1 converges to v_{ss} after short transients due to the interaction with the rest of the group. This is also evident from Fig. 6(c) where the superimposition of the velocities of all the agents (leader included) is shown: one can then verify that all the UAV/UGV velocities converge to the same steady-state value v_{ss}. In order to quantify this convergence, we show in Fig. 6(d) the norm of $e_v = v - \mathbf{1}_{N_3} v_{ss}$, i.e., the velocity error of the overall slave-side w.r.t. the steady-state value v_{ss}. As expected, $\|e_v\|$ goes to zero whenever the master command r_M is kept constant. Finally, figure 6(e) reports the behavior of F_m over time: one can note that F_m (dashed lines) converges to the predicted steady-state value of Prop. 6 (solid lines). As explained in the previous Section, this force cue is useful to inform the operator about the absolute velocity and total number of agents being teleoperated.

In the second HHL simulation, we report the teleoperation of 8 mobile robots (1 leader and 7 followers) moving in an environment cluttered with obstacles, thus enabling the possibility of several split and rejoin decisions. We set

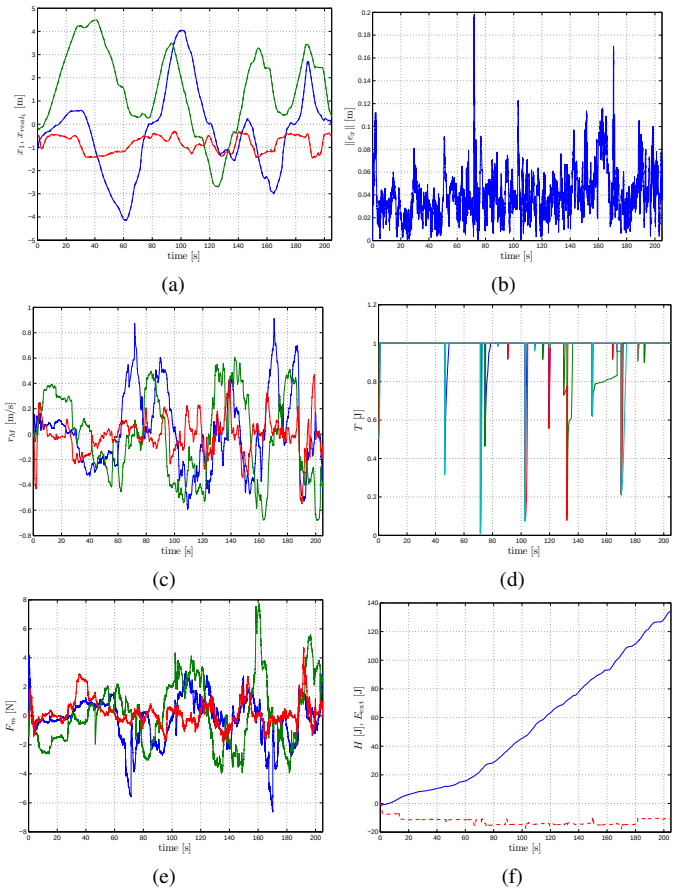

Fig. 8: Results of a representative experiment: a) behavior of the 3 components of the positions x_1 of the leader agent (solid line) and $x_{1,\text{real}}$ of the associated robot (dashed line) — note how they almost perfectly overlap; b) behavior of $\|e_x\|$, the average norm of the tracking errors $x_i - x_{i,real}$: note how this quantity keeps very small over time, indicating an overall good tracking performance of the quadrotors w.r.t. the assumed dynamics (1); c) velocity command $r_M(t)$ set by the human operator (three components, x blue, y green, z red); d) behavior of the tank energies $T(t)$ over time during several split and join decisions; e) the components of the 3D force $F_m(t)$ applied to the master because of the interaction with the slave; f) behavior of $E_{\text{ext}}t)$ (blue line) $E_{\text{in}}(t)$ (red line).

$\bar{T}_i = 8$ [J] as maximum value for the tank energies T_i. Figure 7(a) shows the evolution of the 8 reservoirs T_i from which one can appreciate the several negative jumps due to the execution of the `PassiveJoin` Procedure. We also show in Figs 7(b-c) a detailed view of the tank evolutions during a few consecutive consensus phases in which the tank energies are quickly leveled. Finally, Fig. 7(d) shows the behavior of $E_{\text{ext}}(t) = \int_{t_0}^{t} v^T(\tau)F^e(\tau)\text{d}\tau$ (blue line) and $E_{\text{in}}(t) = \mathcal{H}(t) - \mathcal{H}(t_0)$ (dashed red line) over time. One can then check that $E_{in}(t) \leq E_{ext}(t)$, $\forall t \geq t_0$, as required by the slave-side passivity condition (19).

B. Experimental Results

Experiments have been carried on with a team of 4 quadrotors in the environment depicted in Fig. 8e. The results of a representative experiment are shown in Fig. 8. The velocity command $r_M(t)$ set by the human operator is depicted in Fig. 8c, while Fig. 8a illustrates the behavior of the positions x_1 of the leader agent with dynamics (1) (3 solid lines) and the corresponding real positions $x_{1,\text{real}}$ of the associated quadrotor (3 dashed line). As can be noticed, the dashed lines are basically indistinguishable from the solid lines, indicating that the robot could track the 'virtual' position of (1) with a negligible error. Similarly, Fig. 8b shows the behavior of $\|e_x\|$ over time, that is the average norm of the position error $x_i - x_{i,\text{real}}$, $i = 1 \dots 4$: This plot confirms again that the overall tracking performance of the 4 quadrotors w.r.t. their simplified dynamics (1) was quite satisfactory as this error norm keeps small during the whole operation.

Figure 8e shows the force-feedback signal applied to the haptic device computed from (26): here, the largest peaks correspond to the largest mismatches between the commanded and actual leader velocity due to the interaction with the followers and the obstacles. Figure 8d reports the behavior of the tank energies over time during several split and join decisions. Negative jumps in $T_i(t)$ correspond to energy exchanges between tanks and link potentials in order to ensure passivity of the slave-side (see again the `PassiveJoin` Procedure). Finally, Fig. 8f validates the slave side passivity condition (19) also during the experiments, by showing that the energy provided to the system $E_{\text{ext}}(t)$ (blue line) is always lower bounded by $E_{\text{in}}(t) = \mathcal{H}(t) - \mathcal{H}(t_0)$ (red line).

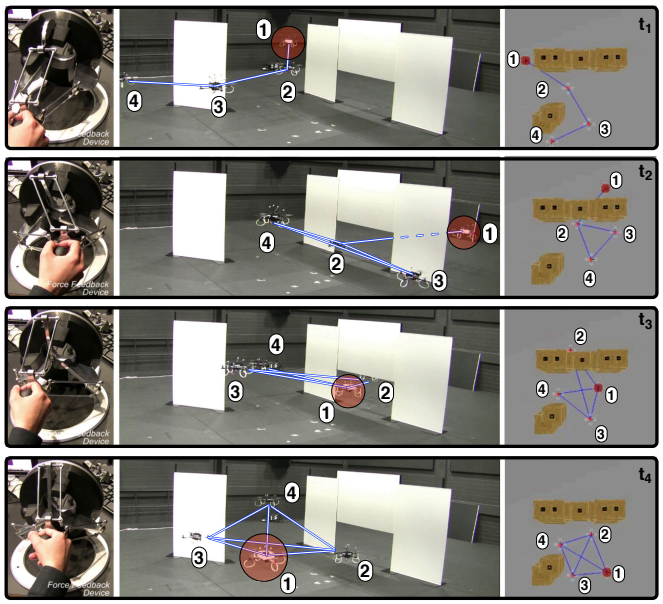

Fig. 9: Each row denotes a different moment of a representative experiment. The left column shows the human operator commanding the leader robot with a 3DOF haptic device. The central column represents 4 UAVs in an environment with obstacles (the white walls with a narrow passage). The right column shows the corresponding top-view in a 3D visualizer. The time-varying interaction graph is enlighten by the presence of blue links representing its edges.

Figure 9 depicts 4 different screenshots of the experiment (the leader robot, agent 1, is encircled by a red ball). The human operator action is shown on the left column while the central column shows the motion of the group and the right column gives a corresponding top-view from a 3D visualizer. The edges of the interaction graph are represented

by blue links: one can appreciate the time-varying nature of the interaction topology since the interconnection graph changes depending on the relative position between robots and because of occlusions by the obstacles. At the beginning (first row) the interaction graph is a chain, while at the end (fourth row) it is a clique (complete graph). The 2 middle rows show again two different graph topologies resulted during the teloperation of the robots. Note how the group is able to seamlessly adapt to the cluttered nature of the environment thanks to its varying interaction topology.

V. Conclusions and Future Work

In this paper we have proposed a decentralized control strategy based on passivity for teleoperating a team of, possibly heterogeneous, mobile robots. By monitoring the exchange of energy among the robots, we were able to obtain a flexible behavior of the group that could smoothly modify the shape of its formation and the communication topology in a stable way. By properly passifying the master robot, a passive bilateral teleoperation system that couples the position of the master to the velocity of the slave side has been developed. The steady-state free motion and contact behaviors of the teleoperation system have been analytically characterized. Finally, the performance of the system has been validated through Human/Hardware-in-the-Loop simulations and real experiments considering a group of UAVs as case study.

In recent works, we considered the issue of connectivity maintenance in the case of distance-visibility neighboring conditions, see [38], and of decentralized velocity synchronization thanks to a suitable variable damping actions, see [39]. We also started to run an extended psychophysical evaluation to study the human perceptual awareness and maneuverability in the teleoperation of a group of mobile robots [40], [41]. As additional extensions of this framework, we are considering the possibility to allow the presence of variable multiple leaders to increase the controllability of the fleet. In the future, we also plan to explicitly take into account inter-robot communication delays so as to formally study the corresponding teleoperation stability issues, and to change online the elasticity of the couplings among the followers in order to adapt the behavior of the group to particular environments or tasks.

Acknowledgements

This research was partly supported by WCU (World Class University) program funded by the Ministry of Education, Science and Technology through the National Research Foundation of Korea (R31-10008). The authors wish to thank Markus Ryll and Johannes Lächele for their assistance in the experimental testbed and the setup of the simulator, respectively.

References

[1] R. M. Murray, "Recent research in cooperative control of multi-vehicle systems," *ASME Journal on Dynamic Systems, Measurement, and Control*, vol. 129, no. 5, pp. 571–583, 2007.

[2] A. Howard, L. E. Parker, and G. S. Sukhatme, "Experiments with a large heterogeneous mobile robot team: Exploration, mapping, deployment and detection," *International Journal of Robotics Research*, vol. 25, no. 5-6, pp. 431–447, 2006.

[3] M. Schwager, D. Rus, and J. J. Slotine, "Decentralized adaptive coverage control for networked robots," *International Journal of Robotics Research*, vol. 28, no. 3, pp. 357–375, 2009.

[4] J. Fink, N. Michael, S. Kim, and V. Kumar, "Planning and control for cooperative manipulation and transportation with aerial robots," *International Journal of Robotics Research*, vol. 30, no. 3, p. 2010, 2010.

[5] N. E. Leonard and E. Fiorelli, "Virtual leaders, artificial potentials and coordinated control of groups," in *40th IEEE Conf. on Decision and Control*, Orlando, FL, Dec. 2001, pp. 2968–2973.

[6] N. Guenard, T. Hamel, and L. Eck, "Control laws for the tele operation of an unmanned aerial vehicle known as an X4-flyer," in *2007 IEEE/RSJ Int. Conf. on Intelligent Robots and Systems*, Beijing, China, Oct. 2006, pp. 3249–3254.

[7] R. Mahony, F. Schill, P. Corke, and Y. S. Oh, "A new framework for force feedback teleoperation of robotic vehicles based on optical flow," in *2009 IEEE Int. Conf. on Robotics and Automation*, Kobe, Japan, May 2009, pp. 1079–1085.

[8] S. Stramigioli, R. Mahony, and P. Corke, "A novel approach to haptic tele-operation of aerial robot vehicles," in *2010 IEEE Int. Conf. on Robotics and Automation*, Anchorage, AK, May 2010, pp. 5302–5308.

[9] B. Hannaford, "Stability and performance tradeoffs in bi-lateral telemanipulation," in *1989 IEEE Int. Conf. on Robotics and Automation*, Scottsdale, AZ, May 1989, pp. 1764–1767.

[10] B. Hannaford, L. Wood, D. A. McAffee, and H. Zak, "Performance evaluation of a six-axis generalized force-reflecting teleoperator," *IEEE Trans. on Systems, Man, & Cybernetics*, vol. 21, no. 3, pp. 620–633, 1991.

[11] T. M. Lam, H. W. Boschloo, M. Mulder, and M. M. V. Paassen, "Artificial force field for haptic feedback in UAV teleoperation," *IEEE Trans. on Systems, Man, & Cybernetics. Part A: Systems & Humans*, vol. 39, no. 6, pp. 1316–1330, 2009.

[12] D. A. Abbink, M. Mulder, F. C. T. van der Helm, M. Mulder, and E. R. Boer, "Measuring neuromuscular control dynamics during car following with continuous haptic feedback," *IEEE Trans. on Systems, Man, & Cybernetics. Part B: Cybernetics*, vol. 41, no. 5, pp. 1239–1249, 2011.

[13] S. Sirouspour, "Modeling and control of cooperative teleoperation systems," *IEEE Trans. on Robotics*, vol. 21, no. 6, pp. 1220–1225, 2005.

[14] D. Lee and M. W. Spong, "Bilateral teleoperation of multiple cooperative robots over delayed communication network: theory," in *2005 IEEE Int. Conf. on Robotics and Automation*, Barcelona, Spain, Apr. 2005, pp. 360–365.

[15] D. Lee, "Semi-autonomous teleoperation of multiple wheeled mobile robots over the internet," in *2008 ASME Dynamic Systems and Control Conference*, Ann Arbor, MI, Oct. 2008.

[16] Y. Cheung and J. S. Chung, "Cooperative control of a multi-arm system using semi-autonomous telemanipulation and adaptive impedance," in *14th Int. Conf. on Robotics*, Munich, Germany, Jun. 2009.

[17] E. J. Rodríguez-Seda, J. J. Troy, C. A. Erignac, P. Murray, D. M. Stipanović, and M. W. Spong, "Bilateral teleoperation of multiple mobile agents: Coordinated motion and collision avoidance," *IEEE Trans. on Control Systems Technology*, vol. 18, no. 4, pp. 984–992, 2010.

[18] D. Lee, A. Franchi, P. Robuffo Giordano, H. I. Son, and H. H. Bülthoff, "Haptic teleoperation of multiple unmanned aerial vehicles over the internet," in *2011 IEEE Int. Conf. on Robotics and Automation*, Shanghai, China, May 2011, pp. 1341–1347.

[19] M. Mesbahi and M. Egerstedt, *Graph Theoretic Methods in Multiagent Networks*, 1st ed., ser. Princeton Series in Applied Mathematics. Princeton University Press, 2010.

[20] H. G. Tanner, A. Jadbabaie, and G. J. Pappas, "Flocking in fixed and switching networks," *IEEE Trans. on Automatic Control*, vol. 52, no. 5, pp. 863–868, 2007.

[21] P. F. Hokayem and M. W. Spong, "Bilateral teleoperation: An historical survey," *Automatica*, vol. 42, no. 12, pp. 2035–2057, 2006.

[22] A. Franchi, P. Robuffo Giordano, C. Secchi, H. I. Son, and H. H. Bülthoff, "A passivity-based decentralized approach for the bilateral teleoperation of a group of UAVs with switching topology," in *2011 IEEE Int. Conf. on Robotics and Automation*, Shanghai, China, May 2011, pp. 898–905.

[23] E. Nuño, L. Basañez, and R. Ortega, "Passivity-based control for bilateral teleoperation: A tutorial," *Automatica*, vol. 47, no. 3, pp. 485–495, 2011.

[24] A. Franchi, H. H. Bülthoff, and P. Robuffo Giordano, "Distributed online leader selection in the bilateral teleoperation of multiple UAVs," in *50th IEEE Conf. on Decision and Control*, Orlando, FL, Dec. 2011, pp. 3559–3565.

[25] M. Fliess, J. Lévine, P. Martin, and P. Rouchon, "Flatness and defect of nonlinear systems: Introductory theory and examples," *International Journal of Control*, vol. 61, no. 6, pp. 1327–1361, 1995.
[26] R. M. Murray, M. Rathinam, and W. Sluis, "Differential flatness of mechanical control systems: A catalog of prototype systems," in *ASME Int. Mechanical Eng. Congress and Exposition*, San Francisco, CA, Nov. 1995.
[27] S. Bouabdallah and R. Siegwart, "Backstepping and sliding-mode techniques applied to an indoor micro," in *2005 IEEE Int. Conf. on Robotics and Automation*, May 2005, pp. 2247–2252.
[28] N. Michael and V. Kumar, "Planning and control of ensembles of robots with non-holonomic constraints," *International Journal of Robotics Research*, vol. 28, no. 8, pp. 962–975, 2009.
[29] I. D. Couzin, "Collective minds," *Nature*, vol. 445, p. 715, 2007.
[30] C. Secchi and C. Fantuzzi, "Formation control over delayed communication networks," in *2008 IEEE Int. Conf. on Robotics and Automation*, Pasadena, CA, May 2008, pp. 563–568.
[31] C. Secchi, S. Stramigioli, and C. Fantuzzi, "Position drift compensation in port-hamiltonian based telemanipulation," in *2007 IEEE/RSJ Int. Conf. on Intelligent Robots and Systems*, Beijing, China, Oct. 2006, pp. 4211–4216.
[32] D. J. Lee and K. Huang, "Passive-set-position-modulation framework for interactive robotic systems," *IEEE Trans. on Robotics*, vol. 26, no. 2, pp. 354–369, 2010.
[33] C. Secchi, S. Stramigioli, and C. Fantuzzi, *Control of Interactive Robotic Interfaces: a port-Hamiltonian Approach*, ser. Tracts in Advanced Robotics. Springer, 2007.
[34] N. Chopra, M. W. Spong, and R. Lozano, "Synchronization of bilateral teleoperators with time delay," *Automatica*, vol. 44, no. 8, pp. 2142–2148, 2008.
[35] C. Secchi, A. Franchi, H. H. Bülthoff, and P. Robuffo Giordano, "Bilateral teleoperation of a group of UAVs with communication delays and switching topology," in *2012 IEEE Int. Conf. on Robotics and Automation*, St. Paul, MN, May 2012.
[36] A. Isidori, *Nonlinear Control Systems, 3rd edition*. Springer, 1995.
[37] G. Niemeyer and J. J. Slotine, "Telemanipulation with time delays," *International Journal of Robotics Research*, vol. 23, no. 9, pp. 873–890, 2004.
[38] P. Robuffo Giordano, A. Franchi, C. Secchi, and H. H. Bülthoff, "Passivity-based decentralized connectivity maintenance in the bilateral teleoperation of multiple UAVs," in *2011 Robotics: Science and Systems*, Los Angeles, CA, Jun. 2011.
[39] ——, "Experiments of passivity-based bilateral aerial teleoperation of a group of UAVs with decentralized velocity synchronization," in *2011 IEEE/RSJ Int. Conf. on Intelligent Robots and Systems*, San Francisco, CA, Sep. 2011, pp. 163–170.
[40] H. I. Son, J. Kim, L. Chuang, A. Franchi, P. Robuffo Giordano, D. Lee, and H. H. Bülthoff, "An evaluation of haptic cues on the tele-operator's perceptual awareness of multiple UAVs' environments," in *IEEE World Haptics Conference*, Istanbul, Turkey, Jun. 2011, pp. 149–154.
[41] H. I. Son, L. L. Chuang, A. Franchi, J. Kim, D. J. Lee, S. W. Lee, H. H. Bülthoff, and P. Robuffo Giordano, "Measuring an operator's maneuverability performance in the haptic teleoperation of multiple robots," in *2011 IEEE/RSJ Int. Conf. on Intelligent Robots and Systems*, San Francisco, CA, Sep. 2011, pp. 3039–3046.

Antonio Franchi (M'07) received the Laurea degree summa cum laude in Electronic Engineering in 2005 and the Ph.D. degree in control and system theory in 2009, both from University of Rome "La Sapienza", Italy.

He is a Research Scientist with the Max Planck Institute for Biological Cybernetics since 2010. He was a visiting student at University of California at Santa Barbara in 2009. His main research interests are in control of autonomous systems and robotics, including planning, cooperative control, estimation, haptics, and human-machine interaction.

Cristian Secchi (M'04) received the Laurea degree in Computer Science Engineering, from the University of Bologna, Italy, in 2000 and the Ph.D. in Information Engineering, from the University of Modena and Reggio Emilia, Italy, in 2004.

He is currently an Assistant Professor with the University of Modena and Reggio Emilia. He has been an Associate Editor of the IEEE Robotics and Automation Magazine from 2006 to 2008 and the Co-Chair of the IEEE Robotics and Automation Society Technical Committee on telerobotics since 2007. His main research interests include teleoperation, mobile robotics, and the control of mechatronic systems.

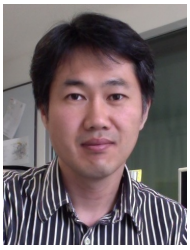

Hyoung Il Son (M'11) received the B.S. and M.S. degrees from the Department of Mechanical Engineering, Pusan National University, Korea, in 1998 and 2000, respectively and the Ph.D. degree from the Department of Mechanical Engineering, KAIST, Korea in 2010.

He is a Research Scientist with the Max Planck Institute for Biological Cybernetics since 2010. He was a senior researcher at LG Electronics (2003-2005) and Samsung Electronics (2005-2009), a research associate at University of Tokyo (2010). His research interests include haptics, teleoperation, psychophysics-based control design and evaluation, and supervisory control of discrete event/hybrid systems.

Heinrich H. Bülthoff (M'96) completed his Ph.D. thesis in Biology at the Eberhard Karls University in Tübingen, Germany in 1980. From 1980 to 1988 he worked as a research scientist at the Max Planck Institute (MPI) for Biological Cybernetics and the Massachusetts Institute of Technology (MIT). He was Assistant, Associate and Full Professor of Cognitive Science at Brown University in Providence from 1988-1993 before becoming director of the Department for Human Perception, Cognition and Action at the MPI for Biological Cybernetics and a scientific member of the Max Planck Society in 1993. He is Honorary Professor at the Eberhard Karls University since 1996 as well as Adjunct Professor at the Korea University (Seoul, Korea). His research interests include object recognition and categorization, perception and action in virtual environments, human-robot interaction and perception.

Paolo Robuffo Giordano (M'08) received the M.Sc. degree in Computer Science Engineering in 2001, and the PhD degree in Systems Engineering in 2008, both from the University of Rome "La Sapienza". In 2007 and 2008 he spent one year as PostDoc at the Institute of Robotics and Mechatronics of the German Aerospace Center, and in 2008 he moved to the Max Planck Institute for Biological Cybernetics where he is currently Senior Research Scientist head of the Human-Robot Interaction group.

His research interests span nonlinear control, robotics, haptics and VR applications.